MOLECULAR AND CELLULAR BIOLOGY, Dec. 2001, p. 8168–8183 Vol. 21, No. 23
0270-7306/01/$04.00+0 DOI: 10.1128/MCB.21.23.8168–8183.2001

Glycosylation Defects and Virulence Phenotypes of *Leishmania mexicana* Phosphomannomutase and Dolicholphosphate-Mannose Synthase Gene Deletion Mutants

ATTILA GARAMI,[1] ANGELA MEHLERT,[2] AND THOMAS ILG[1]*

Max-Planck-Institut für Biologie, Abteilung Membranbiochemie, 72076 Tübingen, Federal Republic of Germany,[1] *and the Division of Molecular Parasitology & Biological Chemistry, Wellcome Trust Biocentre, University of Dundee, DD1 4HN Dundee, Scotland, United Kingdom*[2]

Received 27 June 2001/Accepted 5 September 2001

Leishmania **parasites synthesize an abundance of mannose (Man)-containing glycoconjugates thought to be essential for virulence to the mammalian host and for viability. These glycoconjugates include lipophosphoglycan (LPG), proteophosphoglycans (PPGs), glycosylphosphatidylinositol (GPI)-anchored proteins, glycoinositolphospholipids (GIPLs), and N-glycans. A prerequisite for their biosynthesis is an ample supply of the Man donors GDP-Man and dolicholphosphate-Man. We have cloned from *Leishmania mexicana* the gene encoding the enzyme phosphomannomutase (*PMM*) and the previously described dolicholphosphate-Man synthase gene (*DPMS*) that are involved in Man activation. Surprisingly, gene deletion experiments resulted in viable parasite lines lacking the respective open reading frames (Δ*PMM* and Δ*DPMS*), a result against expectation and in contrast to the lethal phenotype observed in gene deletion experiments with fungi. *L. mexicana* Δ*DPMS* exhibits a selective defect in LPG, protein GPI anchor, and GIPL biosynthesis, but despite the absence of these structures, which have been implicated in parasite virulence and viability, the mutant remains infectious to macrophages and mice. By contrast, *L. mexicana* Δ*PMM* are largely devoid of all known Man-containing glycoconjugates and are unable to establish an infection in mouse macrophages or the living animal. Our results define Man activation leading to GDP-Man as a virulence pathway in *Leishmania*.**

Protozoa of the genus *Leishmania*, which causes a spectrum of diseases in humans, synthesize a range of mannose (Man)-rich glycoconjugates that are secreted by these parasites or form a cell surface glycocalyx. They comprise a number of glycoproteins with conserved GPI anchors and N-glycans as well as the parasite-specific lipophosphoglycans (LPGs), proteophosphoglycans (PPGs), and glycoinositolphospholipids (GIPLs) (Fig. 1A) (8, 17). A prerequisite for the biosynthesis of glycoconjugates in *Leishmania* parasites, like in other eukaryotes, is the conversion of monosaccharides to activated sugar nucleotides and dolicholphosphate derivatives. The activation of Man, which involves the enzymes phosphomannomutase (PMM), GDP-Man pyrophosphorylase (GDPMP), and dolicholphosphate-Man synthase (DPMS), is a crucial biochemical pathway (Fig. 1B), as experiments with *Saccharomyces cerevisiae* demonstrate that these enzymes are essential in this organism (5, 14, 23, 33).

Mammalian and fungal PMMs catalyze the reversible interconversion of Manα1-PO_4 and Man-6-PO_4. They require Manα1,6-bis-PO_4 as cofactor (32) and belong to a novel family of phosphotransferases with the conserved motif DXDX(T/V). The first aspartic acid in this sequence is involved in phosphate transfer and is transiently phosphorylated (4). *S. cerevisiae* PMM was initially identified in a screen for mutations with defects in the secretory pathway as the cytosolic protein Sec53p (23). In humans, two enzymes with PMM activity, PMM1 and PMM2, have been cloned and characterized (27, 28). While PMM1 is also a potent phosphoglucomutase, PMM2 is specific for Man-PO_4 and appears to be the dominant PMM in most human tissues (36).

DPMS is an enzyme associated with the endoplasmic reticulum that forms dolicholphosphate-Man (Dol-P-Man), the second major activated Man derivative used for glycosylation reactions (Fig. 1B). Two different types of DPMS exist in eukaryotes: the enzymes of *S. cerevisiae*, *Trypanosoma brucei*, and *Leishmania mexicana* are formed by a single polypeptide chain, while DPMS from mammals, worms, and *Schizosaccharomyces pombe* is composed of three subunits (26). Mutations in human PMM2 and DPMS lead to the congenital disorders of glycosylation (CDGs) type Ia and Ie, respectively, which are characterized by underglycosylation of many proteins and severe encephalopathy leading to psychomotor retardation (34). Remarkably, among hundreds of mutations, none has been identified that leads to complete abrogation of PMM2 activity, and in CDG type Ie cases, residual DPMS activity is always detectable. The total lack of these two enzymes is considered to be incompatible with human life (34, 37).

Cumulative evidence of a large number of studies over the last 20 years suggests that Man-containing glycoconjugates are required for *Leishmania* viability and virulence in every phase of their life cycle, which includes several promastigote stages in the vector sandflies and the amastigotes in mammalian host macrophages (references 1, 8, 10, and 17 and references therein). It is therefore surprising that the investigation of the Man activation pathway started only very recently. The first components of this pathway identified in *Leishmania* were the Golgi GDP-Man transporter LPG2 (8) and DPMS (22). Gene deletion experiments suggested that DPMS is essential for *Leish-*

* Corresponding author. Mailing address: Max-Planck-Institut für Biologie, Abteilung Membranbiochemie, Corrensstrasse 38, 72076 Tübingen, Federal Republic of Germany. Phone: 49-7071-601238. Fax: 49-7071-601235. E-mail: thomas.ilg@tuebingen.mpg.de.

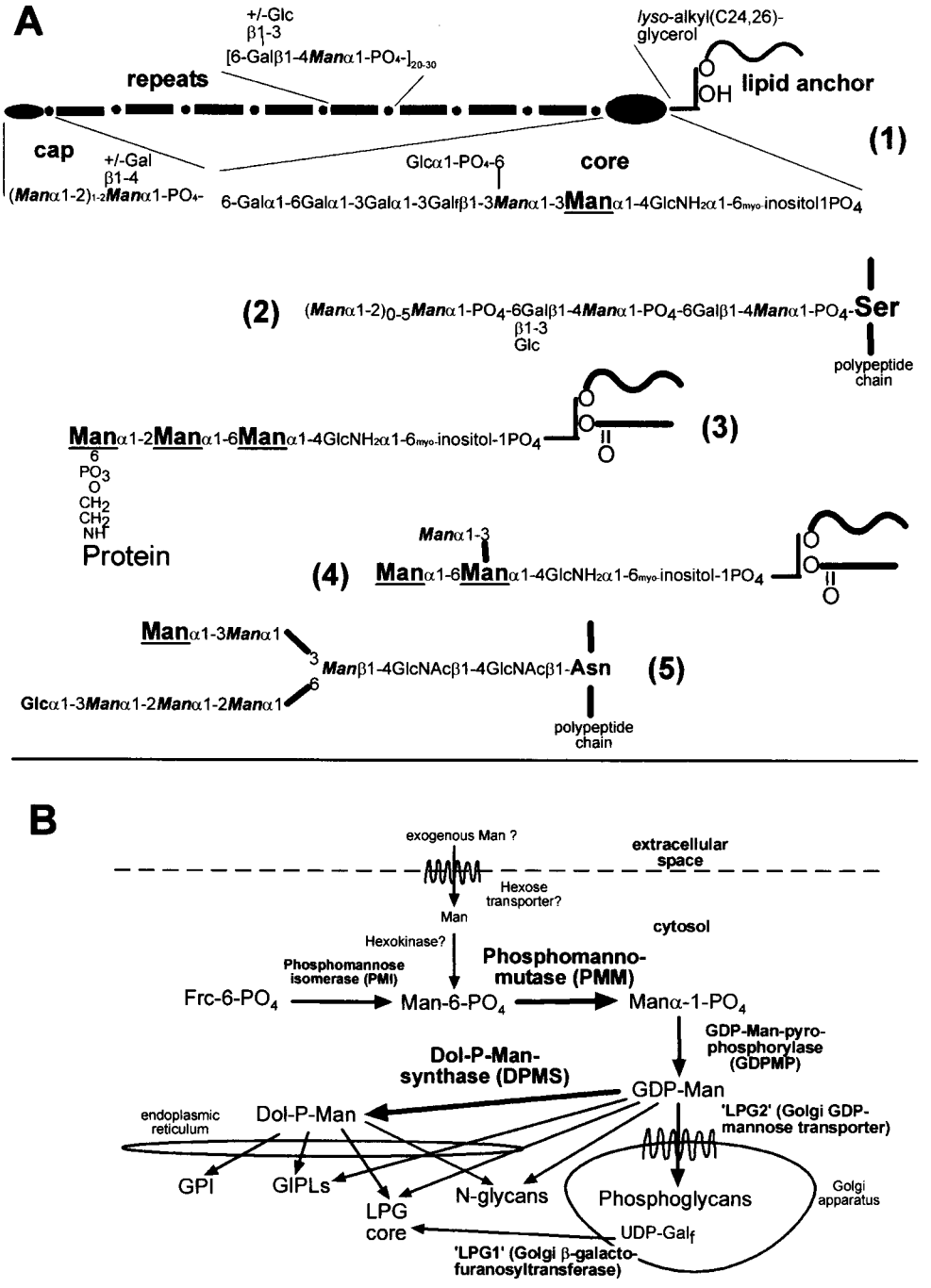

FIG. 1. (A) Structure and biosynthesis of Man-containing *L. mexicana* glycoconjugates. (1), LPG; (2), PPG phosphoglycans; (3), protein GPI anchor; (4), GIPL iM3 (as an example); (5), protein N-glycan. Man residues added from Dol-P-Man are enlarged and underlined, while Man residues added from GDP-Man are in italics and bold. The indication of GDP-Man and Dol-P-Man as Man donors for the biosynthesis of different *Leishmania* glycoconjugates is based on earlier studies (references 8 and 22 and references therein). (B) Man biosynthesis and activation pathways and glycoconjugate synthesis in *L. mexicana*. Bold arrows mark the enzymes that are the topic of this study.

mania viability, and it was concluded that the lethal phenotype is due to the disruption of GIPL biosynthesis in the absence of this enzyme (22). However, a study on phosphomannose isomerase (PMI; Fig. 1B) showed that deletion of its gene in *L. mexicana* leads to dramatic downregulation of glycoconjugate synthesis, including GIPLs, without loss of viability in culture (11). PMI-deficient mutant *L. mexicana* parasites, although attenuated in their infectivity, were still virulent to macrophages and mice. This surprising phenotype may be due to the fact that the lack of PMI and the concomitant glycosylation defect can be bypassed in culture by supplementation with exogenous Man, which is also likely to be present in the host (11).

In this study, we report the cloning of the enzyme in the first

position in the Man activation pathway in *L. mexicana*, the PMM (Fig. 1B), and the generation of gene deletion mutants (Δ*PMM*) which are, in contrast to the corresponding mutant in *S. cerevisiae*, viable in standard growth medium. The surprising existence of a Δ*PMM* mutant suggested that, in contrast to an earlier report, DPMS is unlikely to be essential for *L. mexicana* viability, which was confirmed in this report by the generation of parasite clones lacking the DPMS open reading frame (ORF) (Δ*DPMS*) and detectable DPMS activity. Investigation of glycoconjugate expression and infectivity to macrophages and mice suggests that, in contrast to expectation, the combined absence of LPG, GPI-anchored gp63, and Man-containing GIPLs in *L. mexicana* Δ*DPMS* is not sufficient to abrogate virulence, whereas downregulation of expression of all known Man-containing glycoconjugates in Δ*PMM* parasites leads to an avirulent phenotype.

MATERIALS AND METHODS

Parasite culture and experimental infections of mice and peritoneal macrophages. Promastigotes of the *L. mexicana* wild-type strain MNYC/BZ/62/M379 and derived mutants were grown at 27°C in semidefined medium 79 (SDM) supplemented with 4% heat-inactivated fetal calf serum as described previously (19) and reisolated from mice at 2- to 3-month intervals to preserve virulence. Infection of mice with 10^7 stationary phase promastigotes and infection of mouse peritoneal macrophages were performed as outlined earlier (16). Growth curves of *L. mexicana* wild type and mutants with and without supplementation of the medium with various concentrations of Man (0 μM, 200 μM, and 2 mM) were obtained as previously described (11).

Cloning of *L. mexicana* PMM and DPMS genes, generation of gene knockout and gene addback mutants, heterologous expression of PMM and DPMS, and generation of antibodies. DNA techniques were performed as described previously (13, 20). A 306-bp fragment of the *L. mexicana pmm* gene (*PMM*) was obtained from *L. mexicana* genomic DNA by PCR using the degenerate primers TT(C/T)ATIGA(G/A)TT(C/T)CG(A/G/C/T)AA(C/T)GG(A/G/C/T)ATG and (AG)AAIAT(C/T)TC(A/G)(A/T)A(A/G)TC(A/G)TT(A/G/C/T)CC that were derived from the conserved *S. cerevisiae* (accession number X03213); *Candida albicans* (accession number M96770) and human *pmm1* (accession number U86070) PMM peptide sequences FIEFRNGM and GNDF/YEIF, respectively. The PCR product was subcloned into pGEM-T (Promega) and sequenced. The digoxigenin (DIG)-labeled PCR product was used to screen a λ-Dash-II library (40) derived from genomic *L. mexicana* DNA. Positive clones were subcloned into pBSK$^+$ (Stratagene) or pGEM-5Z (Promega) and sequenced on both strands by the dideoxy chain termination method using an ALFexpress automated sequencer (Amersham-Pharmacia) as described earlier (20). The ORF corresponding to *PMM* was identified by homology to known PMM genes in the database and by determination of the spliced leader site (20). Double targeted gene replacement was performed by PCR amplification of the 5′-untranslated region (5′-UTR) of *PMM* using the primers *pmm*KO1 (AATGCGGCCGC AACGTTGCCATCGCTACTTGGC) and *pmm*KO2 (AGTACTAGTTTTTG CTTTGTTATGGTTTCG) and by amplification of the 3′-UTR of *PMM* using the primers *pmm*KO3 (AGTACTAGTGGATCCATCTCTATCACCACATG TG) and *pmm*KO4 (ATCGATATCAACGTTAGCTAGCAACGCACAAAC). The *Not*I/*Spe*I-cut *PMM* 5′-UTR PCR DNA fragment, the *Bam*HI/*Eco*R V-cut *PMM* 3′-UTR PCR DNA fragment, and a *Spe*I/*Bam*HI DNA fragment containing a hygromycin phosphotransferase gene (*HYG*) (6) were ligated consecutively into pBSK$^+$. For the second *PMM* gene replacement cassette, a *Spe*I/*Bam*HI fragment encoding phleomycin binding protein gene (*BLE*) was used (16). The *HYG*- and *BLE*-containing *PMM* gene replacement cassettes were excised from the plasmids by *Not*I/*Eco*RV digestion and transfected into *L. mexicana* promastigotes as previously described (20). Selection on 96-well microtiter plates and analysis of positive clones were performed as outlined earlier (16). *PMM* 5′-UTR DNA and ORF probes were generated by PCR using a PCR-DIG labeling kit (Roche). For gene addback and heterologous expression studies, the ORF of *PMM* was amplified from a *PMM* gene-containing plasmid using the primers *pmm*ORF1 (GGACTAGTCCCGGGATGGGCTCCAAGGCTATTC) and *pmm*ORF2 (CCGCGGATCCTCACCGCGAATCCTCGAG) and cloned into pGEM-T (Promega). The accuracy of the cloned PCR amplicon was checked by sequencing. Episomal gene addback was achieved by cloning the *Spe*I/*Bam*HI-cut *PMM* ORF into *Xba*I/*Bam*HI-cut pX (24) and transfection of *L. mexicana* Δ*PMM* promastigotes was performed with this construct as described earlier (20). Transfectants were selected by growth in SDM–4% heat-inactivated fetal calf serum containing 10 to 50 μg of G418 (Roche)/ml. Alternatively, the *PMM* gene was expressed under the control of the rRNA promoter by first cloning it into pRIB (11). The *Spe*I/*Bam*HI-excised *PMM*-ORF (see above) was ligated into *Xba*I/*Bgl*II-cut pRIB yielding pRIB*PMM*. For chromosomal integration into the ribosomal locus of *L. mexicana*, the integration cassette was excised by digestion with *Pac*I and *Pme*I (Fig. 3B), gel purified, and transfected into *L. mexicana*. Recombinant clones were isolated by limiting dilution on 96-well plates in SDM containing 20 μg of hygromycin/ml, 2.5 μg of phleomycin/ml, and 20 μM puromycin.

The *L. mexicana* gene encoding DPMS and its 5′-UTR and 3′-UTR sequences were PCR amplified from *L. mexicana* genomic DNA using the primer pairs *dpms*ORF1 and *dpms*ORF2 (GGACTAGTAGATCTATGCAGTACTCCA TTATCG and TCCGGATCCCTGCAGCTAGAAGAGGGAATGGTAG, respectively), *dpms*KO1 and *dpms*KO2 (AATGCGGCCGCGTGATTGGAGC GGC and AGTACTAGTGTTTCCGAGCTAAAACAATG, respectively), and *dpms*KO3 and *dpms*KO4 (TCCGGATCCGCCCCTTGTGCACTCCTGAGC and CTTAAGCTTGCCGCTGCCAGCGTCACCGC, respectively), which were derived from the sequence deposited in the database under the accession number AJ131960 (22). The strategy for the generation of *HYG*- or *BLE*-containing DPMS gene deletion constructs in pBSK was analogous to that employed for *PMM*, except that the restriction enzyme sites of *Bam*HI and *Hin*dIII for the 3′UTR were used. For the generation of *DPMS* gene deletion mutants, the *DPMS* gene replacement cassette (Fig. 3B) was excised by *Not*I/*Hin*dIII digestion. Episomal reexpression was achieved by cloning the *DPMS* ORF into *Bam*HI-cut pX, while reexpression from a ribosomal gene locus (see above) required cloning of the ORF into *Bgl*II-cut pRIB. Orientation of the *DPMS* ORF in both vectors was confirmed by restriction enzyme digests.

Isolation of total RNA from *L. mexicana* promastigotes and mouse lesion-derived amastigotes were described earlier (13). To determine the relative mRNA expression of the PMM and DPMS genes in the two leishmania life stages, reversed transcriptase (RT) PCR was performed using the Titan one tube system (Roche) using the primer pairs CCGTACTCGTTTTTTCAGCAGC AAC and AGTGGAGCGGTAAAGTGAACTTCTC for reverse transcription and amplification of the control *PPG2* mRNAs (13), TCTTCTCTTTGACGT TGATGGCACC and TACGTTGAACATACCGTTGCGGAAC for the *PMM* mRNAs, and TGTCTACAAGCTTGTGATGGATGCC and TGTCTACAAGC TTGTGATGGATGCC for the *DPMS* mRNAs.

High-level expression of *L. mexicana* PMM and DPMS in *Escherichia coli* as inclusion bodies (growth at 37°C) was achieved by cloning a *Bam*HI/*Sal*I-cut *PMM* PCR fragment (primers CCATGGATCCATGGGCTCCAAGGCTATTC and AATGTCGACTCTAGATCACCGCGAATCCTCGAG) and the *Bgl*II/*Pst*I-cut *DPMS* PCR fragment (primers *dpms*ORF1 and *dpms*ORF2) into pQE30, followed by transformation of the bacteria. Inclusion bodies were solubilized in 8 M urea, and the denatured proteins were then purifed by Ni-nitrilotriacetic acid-agarose chromatography as described by the manufacturer (Qiagen). Rabbits were immunized with 200 μg of purified recombinant PMM or DPMS that was dissolved in 8 M urea–50 mM NaH_2PO_4 (pH 4.8) and emulsified with 50% (vol/vol) complete Freund's adjuvant for primary immunizations and with 50% incomplete Freund's adjuvant (vol/vol) for all subsequent booster immunizations. Serum was obtained 10 to 14 days after each booster immunization. Specific antibodies from the anti-PMM and anti-DPMS sera were affinity purified on recombinant PMM or DPMS, respectively, that had been electrotransferred to polyvinylidene difluoride membranes after sodium dodecyl sulfate-polyacrylamide gel electrophoresis (SDS-PAGE) as described earlier (20).

Analytical procedures. Production of SDS-cell lysates, discontinuous SDS-PAGE, immunoblotting using the monoclonal antibodies (MAbs) LT6, LT17, and L7.25 (directed against $[6Gal\beta1\text{-}4Man\alpha1\text{-}PO_4]_x$, $[6(Glc\beta1\text{-}3)Gal\beta1\text{-}4Man\alpha1\text{-}PO_4]_x$ [x = unknown], and $[Man\alpha1\text{-}2]_{0\text{-}2}Man\alpha1\text{-}PO_4$, respectively) (19), affinity-purified rabbit anti-*L. mexicana* SAP antibodies (11), anti-MBAP antibodies (41), anti-*L. mexicana* PMM antibodies, and anti-*L. mexicana* DPMS antibodies (this study), as well as acid phosphatase enzyme assays, were performed as described earlier (16). Stripping of antibodies from immunoblots for reprobing was performed by three 15-min washes in 50 mM Tris-HCl (pH 8.0)–150 mM NaCl–8 M urea–100 mM 2-mercaptoethanol at 65°C. The preparation of lysates, soluble fractions, and washed membranes of promastigotes for SDS-PAGE and immunoblot analysis was performed as described earlier (20).

Total lipids from washed *L. mexicana* promastigotes were obtained by two extractions with $CHCl_3$–CH_3OH–H_2O (4:8:3). High-performance thin-layer chromatography (HPTLC) (Silica60; Merck, Darmstadt, Germany) of total lipids was performed as described earlier (30) using the solvent $CHCl_3$–CH_3OH–1 M NH_4OH (10:10:3). Glycolipids on HPTLC plates were selectively stained by

orcinol/H_2SO_4 spraying. *L. mexicana* promastigotes were metabolically labeled by incubating 5×10^7 cells/ml overnight at 27°C with either 10 μCi of [^{3}H]*myo*-inositol/ml, 20 μCi of [^{3}H]GlcNH$_2$/ml or 50 μCi of 2-[^{3}H]Man (Hartmann Analytics)/ml in *myo*-inositol- or Glc/GlcNH$_2$- or Glc/Man-free SDM, respectively. In labelings with [^{3}H]*myo*-inositol and [^{3}H]GlcNH$_2$, the lipid extracts were further purified by 1-butanol–H_2O phase separation (30). Radioactively labeled lipids of the 1-butanol phase were separated by HPTLC and detected by spraying with ^{3}H-EnHance (Dupont) followed by fluorography. [^{3}H]*myo*-inositol-labeled delipidated cells were incubated with benzonuclease to cleave nucleic acids (20) and then separated by SDS-PAGE. Labeled compounds in acrylamide gels were detected by immersion of the polyacrylamide gel in Amplify (Amersham-Pharmacia), followed by drying and fluorography.

For hexose analysis, 5×10^8 promastigotes were washed three times with phosphate-buffered saline and lysed by resuspension in 1 ml of H_2O and sonication. After centrifugation at 10,000 × *g* for 30 min, the membrane-containing pellet was resuspended in 300 μl of 2 M trifluoroacetic acid and hydrolyzed for 2.5 h at 100°C. After evaporation of the 2 M trifluoroacetic acid, the samples were resuspended in 1 ml of H_2O, delipidated by passage through a Sep-Pac C_{18} column (Waters), and lyophilized. The hexoses of samples equivalent to 10^8 promastigotes were analyzed by gas chromatography-mass spectrometry after methanolysis and trimethylsilylation using *scyllo*-inositol as an internal standard (9).

Enzyme assays of *L. mexicana* PMM and DPMS. Enzyme assays were performed at room temperature in 1 ml of 50 mM triethylamine/HCl (pH 7.0)–0.1 mM EDTA–2.5 mM $MgCl_2$–0.1% bovine serum albumin. For PMM assays, this buffer was supplemented with 0.5 mM $NADP^+$ (Roche), 1 mM 2-mercaptoethanol, 10 μM Glcα1,6$(PO_4)_2$, 1 U of PMI (Sigma)/ml, 1 U of phosphoglucose isomerase (Roche)/ml, and 2 U of glucose-6-phosphate dehydrogenase (Roche)/ml. After addition of sample (2.5 to 20 μl), the rate of background reactions as indicated by the increase in absorbance at 340 nm was recorded for 2 min. The specific PMM assay was initiated by the addition of Manα1-PO_4 (Sigma) to a final concentration of 2 mM and absorbance at 340 nm was recorded for 10 to 15 min. Like yeast PMM (32), *L. mexicana* PMM showed an initial lag phase of activity that was followed by a linear phase, which was used to calculate enzyme activities. Hexokinase and phosphomannose isomerase activity was determined as described earlier (11). One unit of enzyme activity is defined as the amount of enzyme converting 1 μmol of substrate/min into the respective product. An assay for the detection of dolicholphosphate-mannose synthase (DPMS) activity was adapted from an earlier study (25). Then, 2×10^9 promastigotes phosphate-buffered saline-washed promastigotes were resuspended in 1 ml of buffer A (50 mM HEPES/NaOH [pH 7.4], 25 mM KCl, 5 mM $MgCl_2$, 5 mM $MnCl_2$, 2 μg of leupeptin/ml) and disrupted by sonication. Large cell debris was removed by centrifugation at 1,500 × *g* 4°C (10 min), and the supernatant was then centrifuged at 100,000 × *g* for 1 h at 4°C. The microsome-containing pellet was resuspended in 100 μl of buffer A. A dried film of 10 μg of dolichol (C_{55}; Sigma) was resuspended with 20 μl of microsome suspension, 2 μl of CTP (50 mM), and 20 μl of GDP-[^{14}C]Man (NEN) (12.5 μCi/ml in buffer A; final concentration, 18 μM). After incubation for 30 min at 30°C, the reaction was terminated by the addition of 107 μl of CH_3OH and 53.4 μl of $CHCl_3$. Insoluble compounds were removed by centrifugation, the $CHCl_3$–CH_3OH–H_2O extract was dried in a Speedvac and resuspended in $CHCl_3$–CH_3OH–H_2O (4:8:3), and the radioactivity of aliquots was determined by liquid scintillation counting. Total protein of cell lysates was estimated according to Peterson (35).

Immunofluorescence microscopy and FACS of *Leishmania* promastigotes. Immunofluorescence microscopy and fluorescence-activated cell sorting (FACS) studies on *Leishmania* promastigotes and infected macrophages were performed as described previously (16) with the MAbs LT6, L7.25, and LT17 (19; for specificity, see above), MAb L3.8 directed against a polypeptide epitope of *L. mexicana* leishmanolysin/gp63, and the biotinylated lectins concanavalin A (ConA) and Ricin$_{120}$ (Sigma). The MAbs were diluted 1:2 to 1:10 (hybridoma supernatant) or 1:500 to 1:2,000 (ascites fluid), and the lectins were used at 10 μg/ml. Bound MAbs and the biotinylated lectin were detected by incubation with Cy3-labeled goat anti-mouse immunoglobulin G (IgG)/IgM (1:250; Dianova) and fluorescein isothiocyanate-labeled streptavidin (1:250; Sigma), respectively.

Nucleotide sequence accession number. The sequence data for the *PMM*-containing genomic DNA fragment have been submitted to the EMBL database under accession number AJ308232.

RESULTS

Cloning of the PMM gene from *L. mexicana*. A degenerate DNA primer pair was constructed from the conserved PMM peptide sequences FIEFRNGM and GNDF/YEIF/Y (Fig. 2),

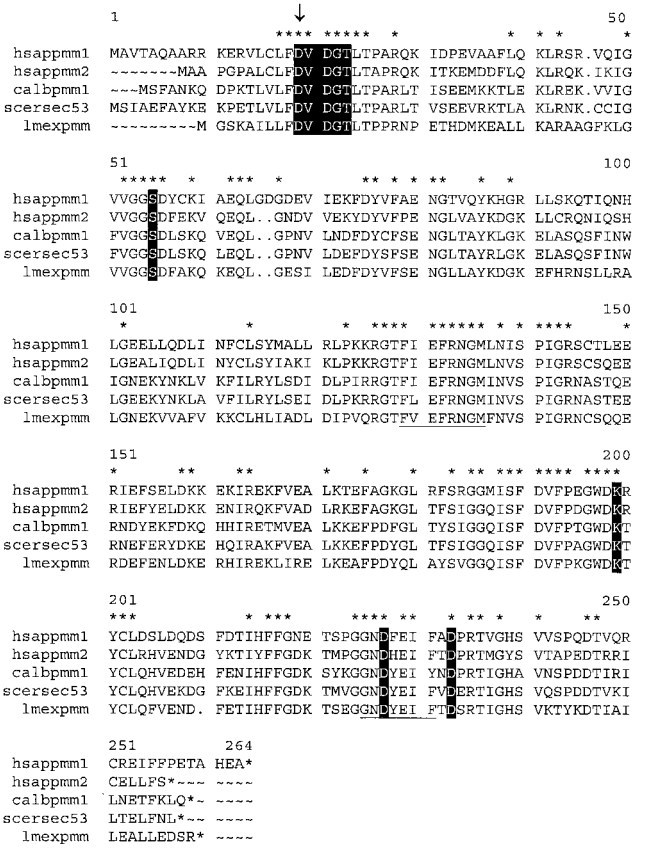

FIG. 2. Alignment of *L. mexicana* PMM (lmexpmm) with amino acid sequences from various organisms: *H. sapiens* PMM1 and PMM2 (hsappmm1 and hsappmm2; 27, 28); *C. albicans* PMM (calbpmm1); *S. cerevisiae* Sec53p (scersec53; 23). Amino acids conserved in PMM of all four species are indicated by stars above the respective amino acids. Residues conserved in this new family of phosphotransferases that has been defined recently (4) are in white letters on black background, and the aspartic acid residue involved in catalysis (4) is marked by an arrow. Amino acid sequences used for the construction of degenerate oligonucleotide primers are underlined.

and PCR was performed using *L. mexicana* genomic DNA as template. The resulting PCR product was sequenced, an ORF was identified with high homology to known PMMs, and this DIG-labeled PCR fragment was used to screen a λ-DashII library of genomic *L. mexicana* DNA. Sequencing of a *PMM* gene-containing DNA fragment (Fig. 3A) revealed an ORF of 744 bp encoding a protein with a molecular mass of ~27.5 kDa (Fig. 2). The predicted polypeptide sequence of *L. mexicana* PMM showed between 52 and 61% identity to PMMs from other eukaryotes like *S. cerevisiae*, *C. albicans*, and *Homo sapiens*. Furthermore, *L. mexicana* PMM contained the amino-terminal DXDX(T/V) motif of phosphotransferases with the conserved aspartic acid residue (D_{10}), which in human PMM was shown to be phosphorylated and involved in phosphate transfer (4) (Fig. 2). Southern blot analysis of *L. mexicana* genomic DNA suggests that *PMM* is a single copy gene (Fig. 4A and data not shown). RT-PCR on promastigote and amastigote total RNA (Fig. 4B) suggests that *PMM* mRNA is present in both parasite life stages but is more abundant in the forms occurring in the mammalian host, the amastigotes. However, immunoblot experiments on parasite total-cell lysates

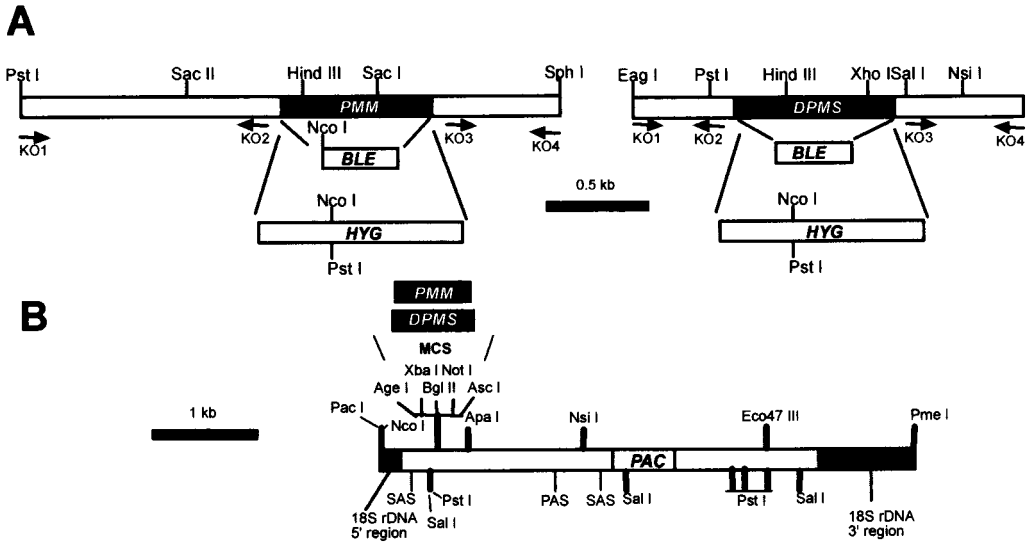

FIG. 3. Targeted gene replacement and gene addback of the *PMM* and *DPMS* alleles. (A) Restriction maps of the *PMM* and *DPMS* loci. The resistance genes *BLE* and *HYG* and the primer binding sites (KO1 to KO4) used for the construction of gene deletion cassettes are indicated. (B) Restriction map of the chromosomal gene addback cassette for genetic rescue of the *L. mexicana* Δ*PMM* and Δ*DPMS* mutants.

probed with antibodies directed against recombinant PMM suggest approximately equal abundance of this enzyme in both life stages (Fig. 5A). *L. mexicana* PMM is not membrane associated, as its activity is largely (>95%) soluble after disruption of promastigotes followed by ultracentrifugation. This result was confirmed by immunoblottings of *L. mexicana* soluble and membrane fractions (Fig. 5B) and by immunofluorescence experiments using affinity-purified anti-PMM antibodies, which suggest a cytoplasmic localization of the enzyme (data not shown).

Targeted gene replacement of PMM in *L. mexicana*. Deletion of the single-copy PMM gene in *S. cerevisiae* is lethal, and it is generally assumed that this is also the case in other eukaryotes, like humans, where partial PMM deficiencies lead to severe disease (34). Surprisingly however, when two rounds of targeted *PMM* gene replacement using the antibiotic resistance markers *HYG* and *BLE* were performed on *L. mexicana* cells (Fig. 3A, left), a series of clones was isolated that lacked both alleles of the *PMM* ORF (*L. mexicana* Δ*PMM::HYG* Δ*PMM::BLE*, further on referred to as Δ*PMM*) (Fig. 4A, lanes 2). These clones were viable in standard culture medium and showed only a mild growth defect compared to wild-type parasites, which could not be rescued by Man supplementation of the medium (Fig. 6C). The absence of the *L. mexicana* Δ*PMM* gene product was confirmed by immunoblottings of total-cell lysates (Fig. 4C). In enzyme assays, the *L. mexicana* Δ*PMM* mutant showed markedly lowered PMM enzyme activity levels, with less than 10% of its specific activity remaining in total-cell lysates, while other hexose metabolism enzymes that use Man as a substrate, like phosphomannose isomerase and hexokinase, were either unaffected by the PMM gene deletion or even upregulated in their activity (Fig. 6A).

General downregulation of Man-containing glycoproteins and glycolipids in *L. mexicana* ΔPMM. Manα1-PO_4, the product of PMM, is the substrate for GDP-Man formation, which is directly or indirectly the sole Man donor for glycoconjugate synthesis in *Leishmania* (reference 22 and references therein; Fig. 1B). A possible defect in the biosynthesis of GDP-Man in *L. mexicana* Δ*PMM* mutants is therefore expected to have a broader impact on the biosynthesis of Man-containing glycoconjugates. Analysis of Δ*PMM* clones suggested downregulated expression of all known lipid- and protein-bound Man-containing glycoconjugates: expression of LPG and phosphoglycan caps and repeats of PPGs was either absent or very low as judged by the lack of specific bands with the anti-phosphodisaccharide repeat MAb LT6 (Fig. 4D) and the downregulation of binding sites for the anti-phosphotrisaccharide repeat MAb LT17 as well as the anti-phosphoglycan cap MAb L7.25 on immunoblots of total promastigote lysates (Fig. 4E and F), the absence of surface and flagellar pocket signals in immunofluorescence experiments (Fig. 7A and B), absence or severe downregulation of FACS signals in labelings of live cells with the MAbs LT6 and LT17 (Fig. 7J and L), the lack of detectable LPG in metabolic [^{3}H]inositol labelings (Fig. 5C), and the absence of LPG in attempted purifications by a standard protocol (not shown; see reference 29). Δ*PMM* promastigotes downregulated the surface expression of GPI-anchored gp63 (Fig. 7D, E, and K), and no [^{3}H]inositol-labeled gp63 was detected after metabolic labeling (Fig. 5C), suggesting that protein GPI anchor synthesis was also affected in the mutant parasites. Evidence for a defect in N-glycosylation was obtained by immunoblottings of *L. mexicana* wild-type and Δ*PMM* total-cell lysates, where a mobility shift of ~15 kDa for the normally heavily N-glycosylated MBAP (31, 41) was observed in the mutant (Fig. 5D, lanes 1 and 2), which is indicative of the loss of N-glycans in this molecule. The Man-containing GIPLs were undetectable in *L. mexicana* Δ*PMM* in HPTLC-separated total lipids by either orcinol staining or by fluorography after metabolic labeling with [^{3}H]Man, [^{3}H]$GlcNH_2$, and [^{3}H]*myo*-inositol (Fig. 5E to H). In fluorescence microscopy and FACS analyses, Δ*PMM* promastigotes showed only a very weak signal (Fig. 7G, H, and M) with ConA, a lectin that strongly binds to α-Man residues (7) present in *L. mexicana* N-glycans, LPG, PPGs, and GIPLs (8, 16, 17, 21). Finally,

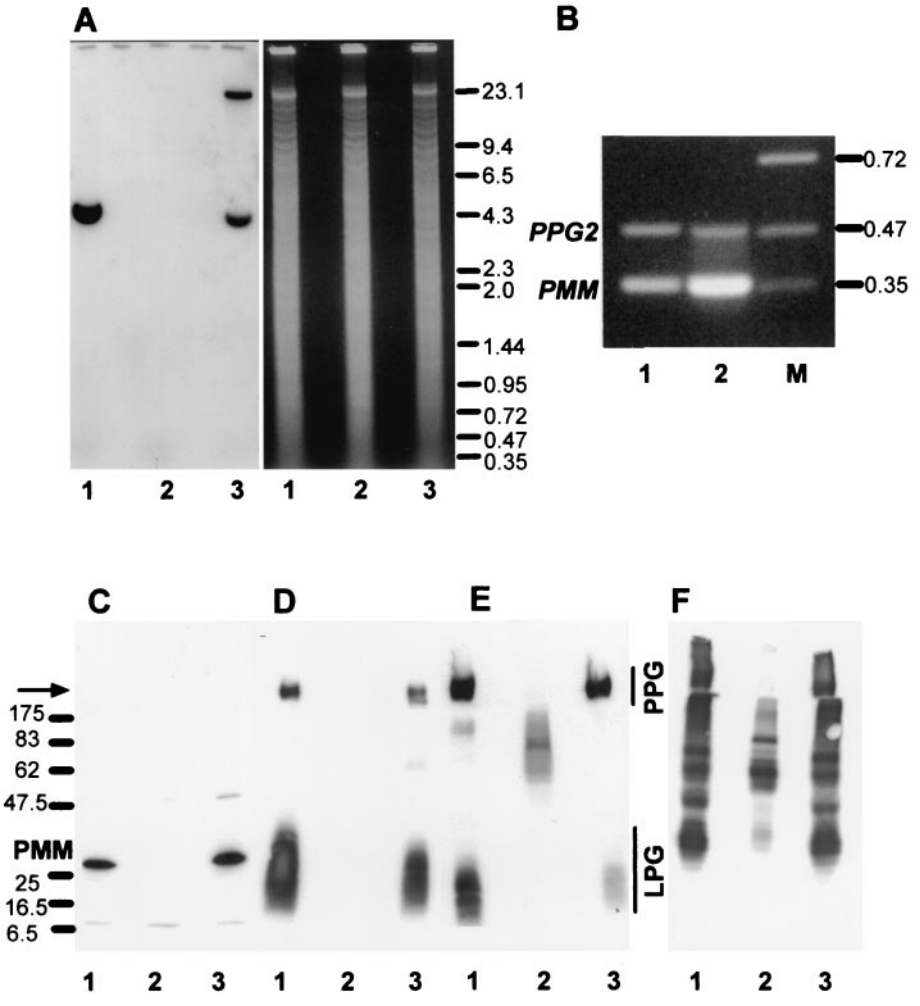

FIG. 4. Analysis of *L. mexicana* wild type, a Δ*PMM* mutant, and a *PMM* gene addback mutant by Southern blotting, RT-PCR, and immunoblotting. (A) Southern blot analysis of *Pst*I restriction enzyme-digested chromosomal DNA (10 μg) from *L. mexicana* wild type (lanes 1), a Δ*PMM* mutant (lanes 2). and a Δ*PMM* + cRIB*PMM* gene addback mutant (lanes 3). The digested DNAs were separated on an ethidium bromide-containing 0.7% agarose gel (right), blotted onto a nylon membrane, and incubated with a DIG-labeled *PMM* ORF probe (left). The sizes of DNA standards are indicated in kilobases. (B) Amplification of *PMM* mRNA from *L. mexicana* log-phase promastigote (lane 1) and amastigote (lane 2) by RT-PCR from total RNA. The loading was normalized to the coamplified cDNA fragment derived from the *PPG2* gene, whose mRNA is approximately equally abundant in *L. mexicana* promastigotes and amastigotes (13). The sizes of DNA standards (lane M) are indicated in kilobases. (C to F) SDS-PAGE and immunoblotting of *L. mexicana* wild type and Δ*PMM* mutant total-cell lysates. Lanes 1, wild type; lanes 2, Δ*PMM*; lanes 3, Δ*PMM* + cRIB*PMM*. Each lane was loaded with 10^6 promastigotes (~4 μg of protein). (C) Blot was probed with affinity-purified rabbit anti-*L. mexicana* PMM antibodies. The same or identically loaded blots were then stripped and probed with MAb LT6 (directed against $[6Gal\beta1\text{-}4Man\alpha1\text{-}PO_4]_x$) (D), LT17(directed against $[6(Glc\beta1\text{-}3)Gal\beta1\text{-}4Man\alpha1\text{-}PO_4]_x$ [x = unknown]) (E), and MAb L7.25 (directed against $[Man\alpha1\text{-}2]_{0\text{-}2}Man\alpha1\text{-}PO_4$) (F). The molecular masses and relative positions of standard proteins and the positions of PMM, LPG, and PPG are indicated. The arrow marks the border between stacking and separating gels.

hexose analysis of trifluoroacetic acid-hydrolyzed promastigote membranes by gas chromatography-mass spectrometry showed that the amount of macromolecule-associated Man in *L. mexicana* Δ*PMM* was below the detection limit of the method (Fig. 6D).

The profound glycosylation defects in *L. mexicana* Δ*PMM* promastigotes were caused by the absence of the PMM gene, since *PMM* addback by integration into a rRNA gene locus (Fig. 3B), which resulted unexpectedly in the integration of two gene copies (Fig. 4A, lane 3), or by an episomal vector (pX; not shown) reconstituted the synthesis of all glycoconjugates investigated in this study (Fig. 4C to F, lanes 3; Fig. 5C, D, and H, lanes 3; Fig. 7C, F, I, and J to M).

Targeted gene replacement of DPMS in *L. mexicana*. DPMS has been reported to be an essential enzyme for *S. cerevisiae* (33) and *S. pombe* (5). The DPMS gene (*DPMS*) of *L. mexicana* has recently been cloned and sequenced, and it has been reported that this enzyme is essential for the parasite (22). However, the unexpectedly successful generation of the *L. mexicana PMM* gene deletion mutants led us to the conclusion that in contrast to the previous report, *DPMS* may also not be required for *L. mexicana* viability in culture. In agreement with this prediction, after cloning the *L. mexicana* single-copy DPMS gene locus by PCR amplification, two rounds of targeted gene replacement (Fig. 3A) resulted in parasite clones lacking both alleles of the *DPMS* ORF (*L. mexicana*

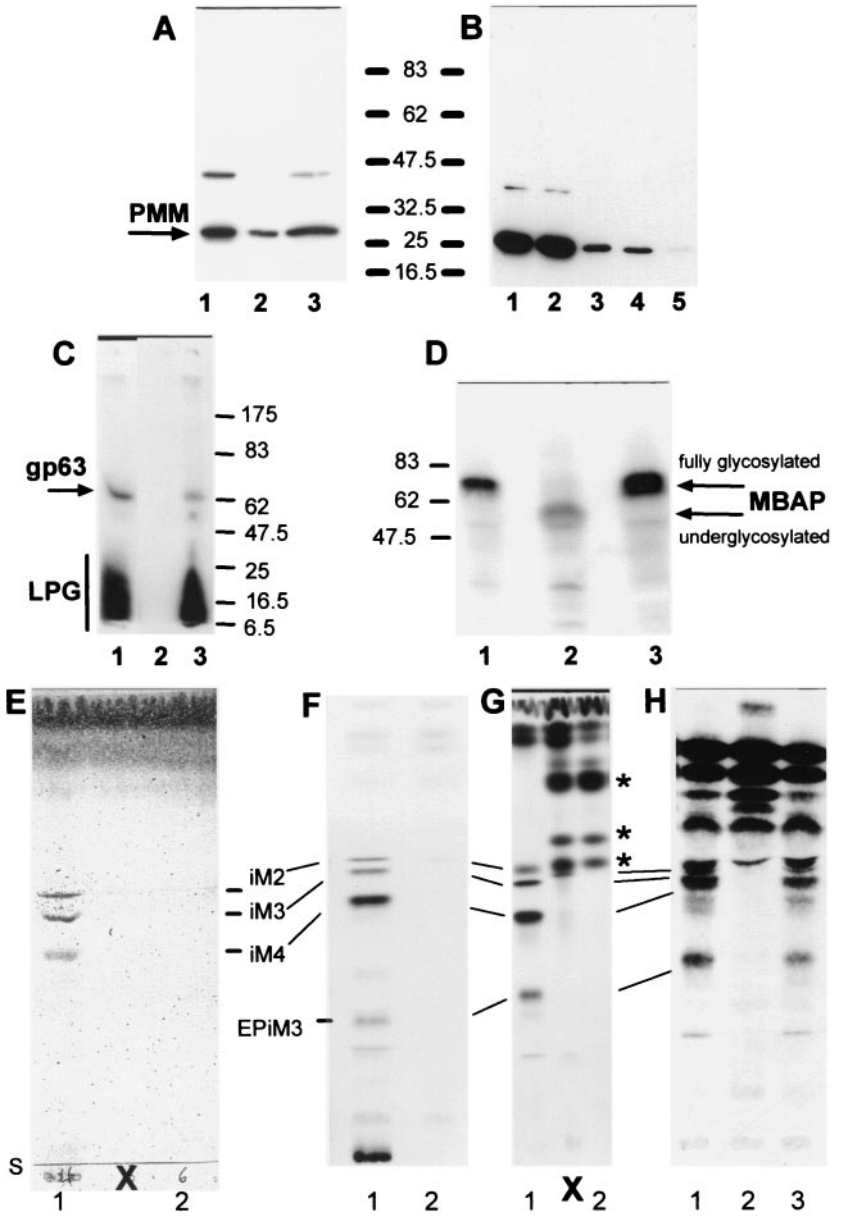

FIG. 5. Analysis of *L. mexicana* wild type, a Δ*PMM* mutant, and a *PMM* gene addback mutant by SDS-PAGE and immunoblotting, SDS-PAGE and fluorography, and TLC analysis. (A) SDS-PAGE and immunoblotting of total-cell lysates of *L. mexicana* promastigotes (lane 1, 2.5×10^6 parasites, corresponding to ~10 μg of protein) and lesion-derived amastigotes (lane 2, 2.5×10^6 parasites, corresponding to ~3.5 μg of protein; lane 3, 7×10^6 parasites, corresponding to ~10 μg of protein). The blots were probed with affinity-purified rabbit anti-*L. mexicana* PMM antibodies. (B) SDS-PAGE and immunoblotting of total-cell lysates of *L. mexicana* promastigotes fractionated by ultracentrifugation: lane 1, total-cell lysate of 2.5×10^6 parasites, corresponding to ~10 μg of protein; lane 2, first ultracentrifugation supernatant; lane 3, first ultracentrifugation pellet; lane 4, second ultracentrifugation supernatant; lane 5, second ultracentrifugation pellet. Equivalent sample volumes were loaded, and the blots were probed with affinity-purified rabbit anti-*L. mexicana* PMM antibodies. (C) SDS-PAGE and fluorography of delipidated total promastigote lysates from [^{3}H]*myo*-inositol-labeled *L. mexicana* wild type (lane 1), Δ*PMM* (lane 2), and Δ*PMM* + cRIBΔ*PMM* (lane 3). Each lane was loaded with 2.5×10^7 delipidated promastigotes labeled overnight with [^{3}H]*myo*-inositol. The positions of ^{14}C-labeled protein markers, LPG, and the major GPI-anchored surface metalloproteinase gp63 are indicated. (D) SDS-PAGE and immunoblotting of promastigote lysates (2×10^7 lysates, corresponding to ~80 μg of protein) of wild type (lane 1), Δ*PMM* (lane 2), and Δ*PMM* + cRIB*PMM* (lane 3). The blots were probed with affinity-purified rabbit anti-*L. mexicana* MBAP antibodies. The molecular masses and relative positions of standard proteins and the positions of PMM and MBAP are indicated (A to D). (E to H) Silica gel 60 HPTLC analysis of the predominant promastigote glycolipids of *L. mexicana* in wild type and Δ*PMM* mutant promastigotes. Lanes 1, wild type; lanes 2, Δ*PMM*; lane 3, Δ*PMM* + cRIB*PMM*. (E) Total lipids from 2×10^8 promastigotes visualized by orcinol/H_2SO_4 spraying. (F) Fluorography of total lipids from 2.5×10^7 [^{3}H]Man-labeled promastigotes (approximately 100,000 cpm). (G) Fluorography of total lipids from 5×10^6 [^{3}H]GlcNH_2-labeled promastigotes (approximately 100,000 cpm). (H) Fluorography of total lipids from 5×10^6 [^{3}H]*myo*-inositol-labeled promastigotes (approximately 100,000 cpm). Bars, positions of abundant *L. mexicana* GIPLs (30); S, start of TLCs; *, new [^{3}H]GlcNH_2-labeled compounds accumulating in the Δ*PMM* mutant; X, two lanes loaded with samples irrelevant to this study.

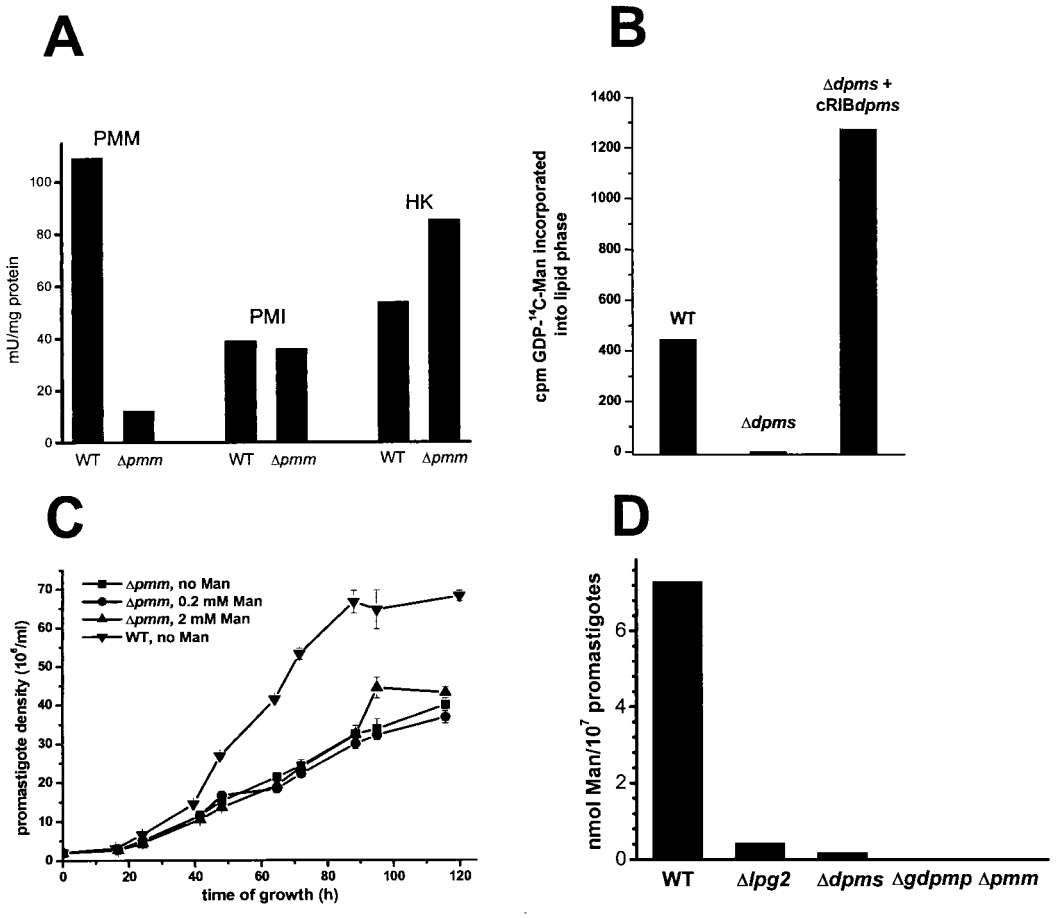

FIG. 6. Enzyme activities, growth curve, and Man content of *L. mexicana* wild-type (WT) and mutant promastigotes. (A) Enzymatic activity of phosphomannomutase (PMM), phosphomannose isomerase (PMI), and hexokinase (HK) in freeze/thaw/sonication lysates of wild-type *L. mexicana* and a Δ*PMM* mutant. (B) Synthesis of lipid-bound [^{14}C]Man by microsomal fractions of *L. mexicana* wild-type, Δ*DPMS*, and Δ*DPMS* + cRIB*DPMS* promastigotes. The bars represent the average of duplicate assays. (C) Growth curves of *L. mexicana* wild-type and Δ*PMM* mutant promastigotes with and without Man supplementation of the medium. (D) Man content of membranes from *L. mexicana* wild-type and several mutant promastigotes, as determined by gas chromatography-mass spectrometry.

Δ*DPMS::HYG* Δ*DPMS::BLE*, further on referred to as Δ*DPMS*) (Fig. 8A). In the case of Δ*DPMS* promastigotes, the 29-kDa DPMS protein band was no longer detectable in immunoblots probed with antibodies raised against the recombinant protein (Fig. 8C). Furthermore, the absence of [^{14}C]Man transfer from GDP-[^{14}C]Man into the lipid fraction of resuspended microsomal pellets in mutant compared to wild-type and *DPMS* gene addback parasites was taken as an indication for the absence of DPMS activity in the mutant (Fig. 6B). Immunoblottings of soluble and membrane fractions of *L. mexicana* promastigotes suggest that DPMS is a membrane-associated protein (Fig. 9B), as predicted by its gene sequence (22). DPMS was expressed in amastigotes, but expression levels of mRNA and protein did not appear to correlate (Fig. 8B and Fig. 9A).

Selective downregulation of Man-containing glycoproteins and glycolipids in *L. mexicana* ΔDPMS. Earlier in vitro studies on microsome fractions suggested that in *L. mexicana*, Dol-P-Man is the α-Man donor for the first Man of the LPG core sequence, the transfer of all three Man residues of protein GPI anchors, the first two Man of the GIPLs, and possibly the Man_6 of N-glycans. By contrast, the synthesis of phosphoglycan chains on both LPG and PPGs and the synthesis of Man_{1-5} of N-glycans require only GDP-Man (22) (Fig. 1A and B). Analysis of glycoconjugate expression in *L. mexicana* Δ*DPMS* is in agreement with the predictions of this scheme: the mutant parasites lack LPG, as indicated by immunoblottings of total-cell lysates probed with the MAbs LT6 and LT17 (Fig. 8D and E), by metabolic labeling with [^{3}H]*myo*-inositol (Fig. 9C), and by unsuccessful attempts to purify the glycolipid by standard methods (not shown) (29). In contrast to LPG biosynthesis, phosphoglycosylation of proteins by phosphoglycan repeats and mannooligosaccharide caps remains normal or is even slightly elevated, as shown by immunoblottings of total-cell lysates (Fig. 8D to F) and of culture supernatant containing the major secreted PPGs SAP and fPPG (data not shown). The lack of LPG on Δ*DPMS* promastigotes was confirmed by the absence of a cell surface signal in immunofluorescence experiments with MAb LT6, while wild-type parasites show the expected intense fluorescence (Fig. 10A and B). Longer exposures of LT6-labeled Δ*DPMS* promastigotes (Fig. 10B′) revealed a fluorescence signal mainly in the secretory organelle,

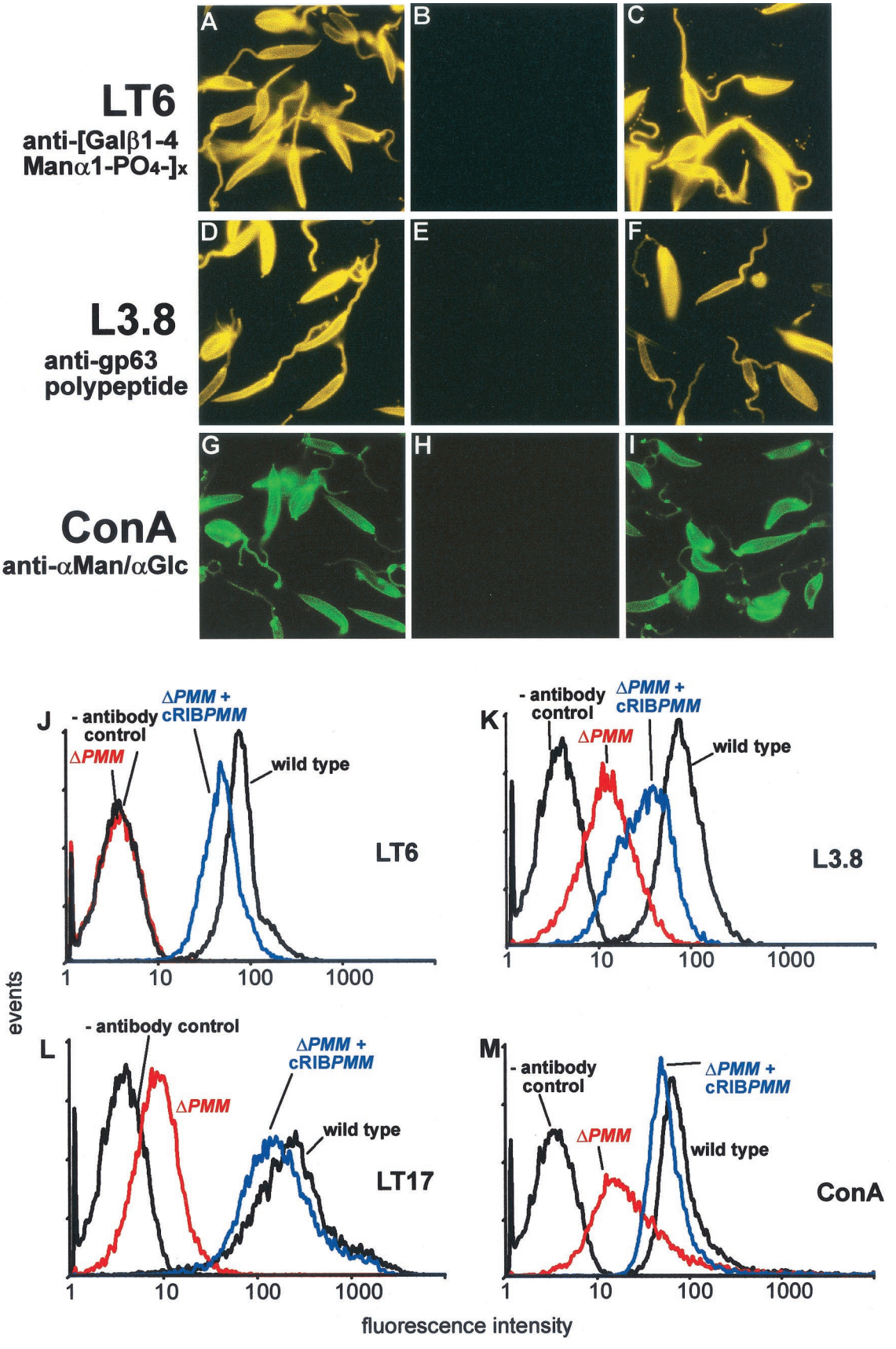

FIG. 7. Immuno-/lectin-fluorescence microscopy and FACS analysis of *Leishmania* wild-type, Δ*PMM* mutant, and *PMM* gene addback mutant promastigotes. (A, D, G) *L. mexicana* wild type; (B, E, H) *L. mexicana* Δ*PMM*; (C, F, I) *L. mexicana* Δ*PMM* + cRIBΔ*PMM*. Exposure times within rows are identical. The cells were not permeabilized after fixation. The MAbs and lectins used are indicated by the labeling of rows. (J to M) FACS analysis of live *L. mexicana* promastigotes. The parasite lines and the MAbs and lectins used are indicated in each panel.

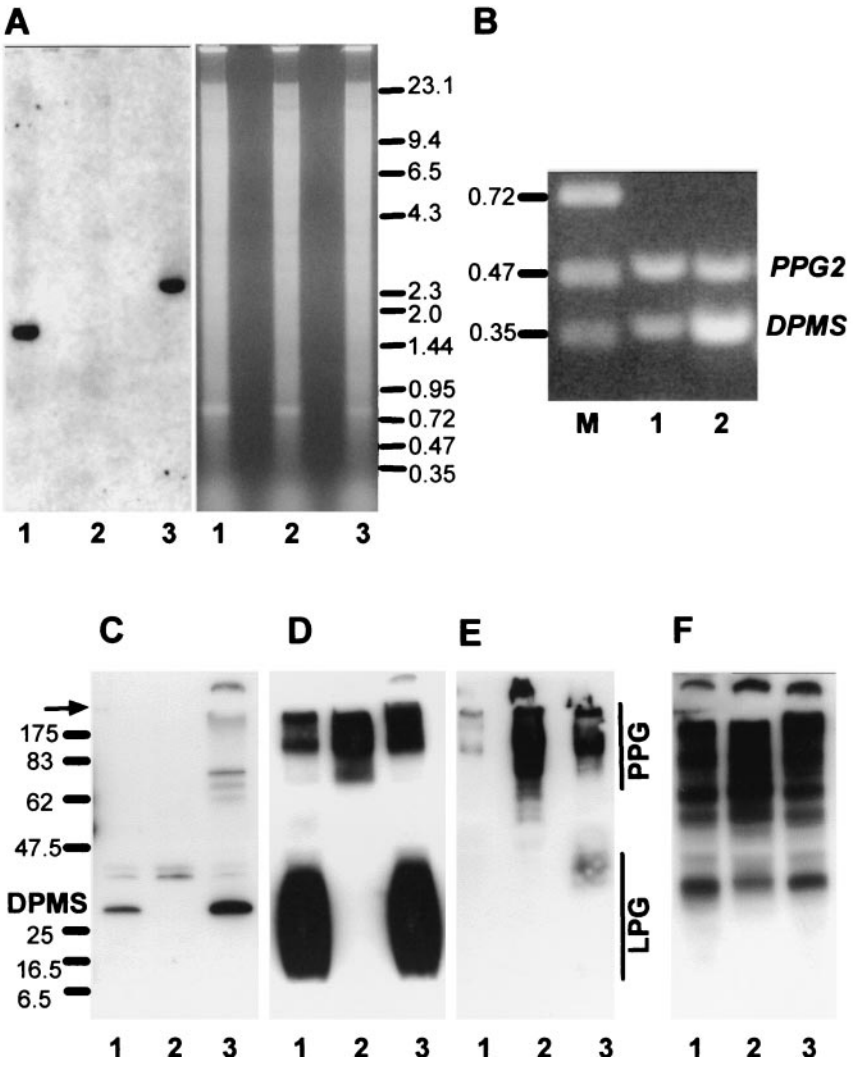

FIG. 8. Analysis of *L. mexicana* wild type, a Δ*DPMS* mutant, and a *DPMS* gene addback mutant by Southern blotting, RT-PCR, and immunoblotting. (A) Southern blot analysis of *Sal*I restriction enzyme-digested chromosomal DNA (10 μg) from *L. mexicana* wild type (lanes 1), a Δ*DPMS* mutant (lanes 2), and a Δ*DPMS* + cRIB*DPMS* gene addback mutant (lanes 3). The digested DNAs were separated on an ethidium bromide-containing 0.7% agarose gel (right), blotted onto a nylon membrane, and incubated with a DIG-labeled *DPMS* ORF probe (left). The sizes of DNA standards are indicated in kilobases. (B) Amplification of *DPMS* mRNA from *L. mexicana* log-phase promastigote (lane 1) and amastigote (lane 2) by RT-PCR from total RNA. The loading was normalized to the coamplified cDNA fragment derived from the *PPG2* gene, whose mRNA is approximately equally abundant in *L. mexicana* promastigotes and amastigotes (13). The sizes of DNA standards are indicated in kilobases. (C to F) SDS-PAGE and immunoblotting of *L. mexicana* wild-type, Δ*DPMS* mutant, and DPMS gene addback total promastigote lysates. Lane 1, wild type; lane 2, Δ*DPMS*; lane 3 Δ*DPMS* + cRIB*DPMS*. Each lane was loaded with 10^6 promastigotes (~4 μg of protein). (C) Blots probed with affinity-purified rabbit anti-*L. mexicana* DPMS antibodies. The same or identically loaded blots were then stripped and probed with MAb LT6 (directed against $[6Gal\beta1\text{-}4Man\alpha1\text{-}PO_4]_x$) (D), MAb LT17(directed against $[6(Glc\beta1\text{-}3)Gal\beta1\text{-}4Man\alpha1\text{-}PO_4]_x$ [x = unknown]) (E), and MAb L7.25 (directed against $[Man\alpha1\text{-}2]_{0\text{-}2}Man\alpha1\text{-}PO_4$) (F). The molecular masses and relative positions of standard proteins and the positions of DPMS, LPG, and PPG are indicated. The arrow marks the borders between stacking and separating gels.

the flagellar pocket. This weak immunofluorescence signal (Fig. 10B′), which was barely detectable by FACS (Fig. 10J), was most likely due to the secretion of phosphoglycosylated SAP and fPPG (39), whose glycan modifications are unaffected by the defect in dolicholphosphate-mannose synthesis (Fig. 1A and B). In contrast to MAb LT6, MAb LT17, which reacts more strongly with PPGs versus LPG (16; compare also Fig. 8E), showed a cell surface FACS signal (Fig. 10L) and immunofluorescence signal (not shown) with Δ*DPMS* promastigotes. This cell surface binding of LT17 to the LPG-deficient Δ*DPMS* promastigotes was about 10-fold weaker than that observed on LPG-expressing wild-type cells (Fig. 10L) and most likely corresponded to surface-expressed PPGs (Fig. 8E).

Surface expression of the dominant *Leishmania* surface protein, the GPI-anchored metalloproteinase gp63, is undetectable by immunofluorescence labeling of nonpermeabilized fixed Δ*DPMS* promastigotes (compare Fig. 10D and E) and FACS analysis of live cells (Fig. 10K). Immunofluorescence labeling of permeabilized Δ*DPMS* promastigotes reveals intracellular staining that is often intense around the nucleus, sug-

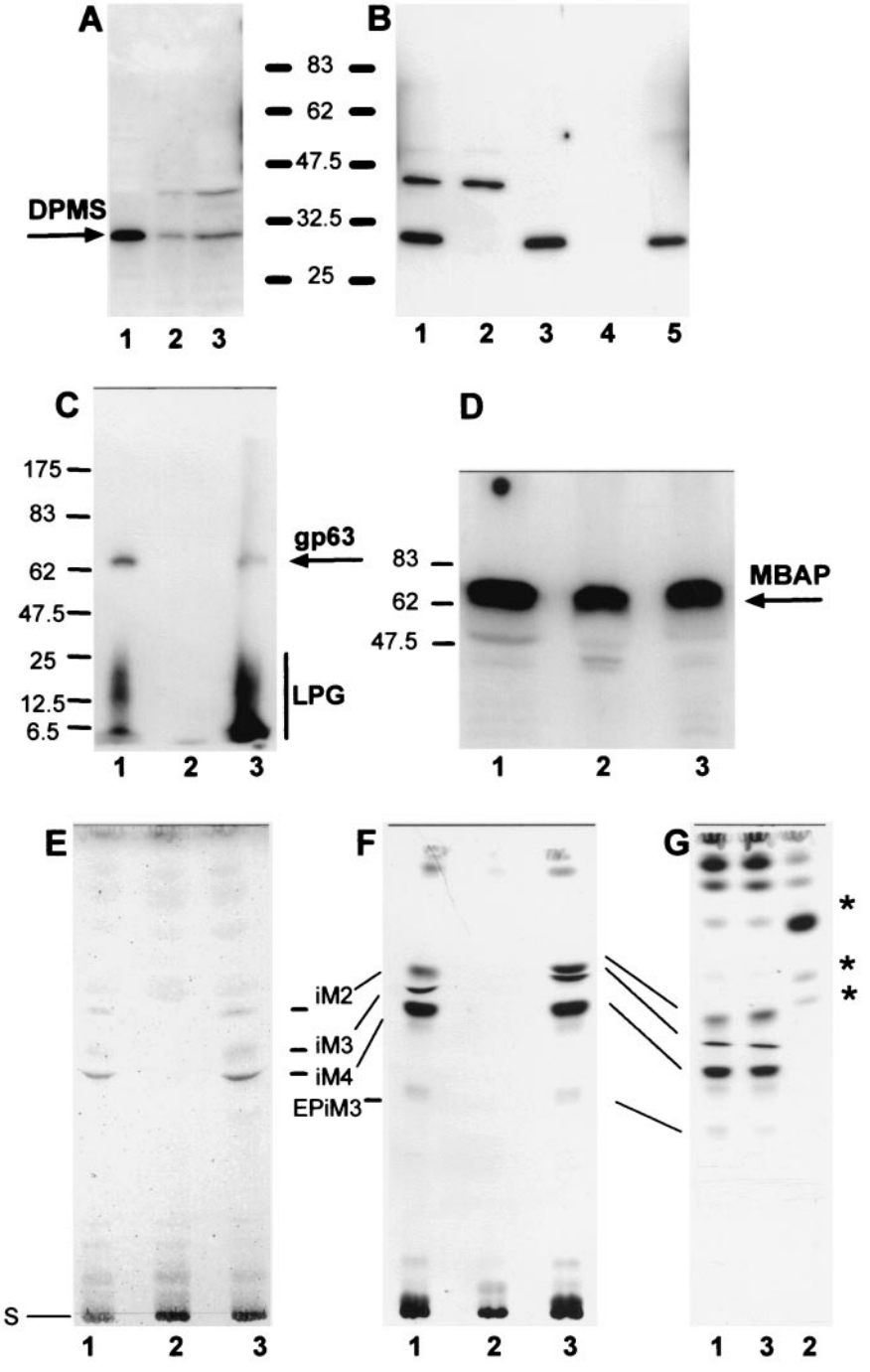

FIG. 9. Analysis of *L. mexicana* wild type, a Δ*DPMS* mutant, and a *DPMS* gene addback mutant by SDS-PAGE and immunoblotting, SDS-PAGE and fluorography, and TLC analysis. (A) SDS-PAGE and immunoblotting of total-cell lysates of *L. mexicana* promastigotes (lane 1, 2.5×10^6 parasites, corresponding to ~10 μg of protein) and lesion-derived amastigotes (lane 2, 2.5×10^6 parasites, corresponding to ~3.5 μg of protein; lane 3, 7×10^6 parasites, corresponding to ~10 μg of protein). The blots were probed with affinity-purified rabbit anti-*L. mexicana* DPMS antibodies. (B) SDS-PAGE and immunoblotting of total-cell lysates of *L. mexicana* promastigotes fractionated by ultracentrifugation: lane 1, total-cell lysate of 2.5×10^6 parasites, corresponding to ~10 μg of protein; lane 2, first ultracentrifugation supernatant; lane 3, first ultracentrifugation pellet; lane 4, second ultracentrifugation supernatant; lane 5, second ultracentrifugation pellet. Equivalent sample volumes were loaded, and the blots were probed with affinity-purified rabbit anti-*L. mexicana* DPMS antibodies. (C) SDS-PAGE and fluorography of delipidated total promastigote lysates from [^{3}H]*myo*-inositol-labeled *L. mexicana*. Lane 1, wild type; lane 2, Δ*DPMS*; lane 3, Δ*DPMS* + cRIB*DPMS*. Each lane was loaded with 2.5×10^7 delipidated promastigotes labeled overnight with [^{3}H]*myo*-inositol. The positions of ^{14}C-labeled protein markers, LPG ,and the major GPI-anchored surface metalloproteinase gp63 are indicated. (D) SDS-PAGE and immunoblotting of promastigote lysates (2×10^7 lysates, corresponding to ~80 μg of protein). Lane 1, wild type; lane 2, Δ*DPMS*; lane 3, Δ*DPMS* + cRIB*DPMS*. The blots were probed with affinity-purified rabbit anti-*L. mexicana* MBAP antibodies. The molecular masses and relative positions of standard proteins and the positions of DPMS and MBAP are indicated (A to D). (E to G) Silica gel 60 HPTLC analysis of the predominant promastigote glycolipids of *L. mexicana* in wild-type and Δ*DPMS* mutant promastigotes. Lanes 1, wild type; lanes 2, Δ*DPMS*; lanes 3, Δ*DPMS* + cRIB*DPMS*. (E) Total lipids from 2×10^8 promastigotes were visualized by orcinol/H_2SO_4 spraying. (F) Fluorography of total lipids from 2.5×10^7 [^{3}H]Man-labeled promastigotes (approximately 100,000 cpm). (G) Fluorography of total lipids from 5×10^6 [^{3}H]GlcNH_2-labeled promastigotes (approximately 100,000 cpm). Bars, positions of the abundant *L. mexicana* GIPLs (30); S, start of TLCs; *, new [^{3}H]GlcNH_2-labeled compounds accumulating in Δ*DPMS* mutant.

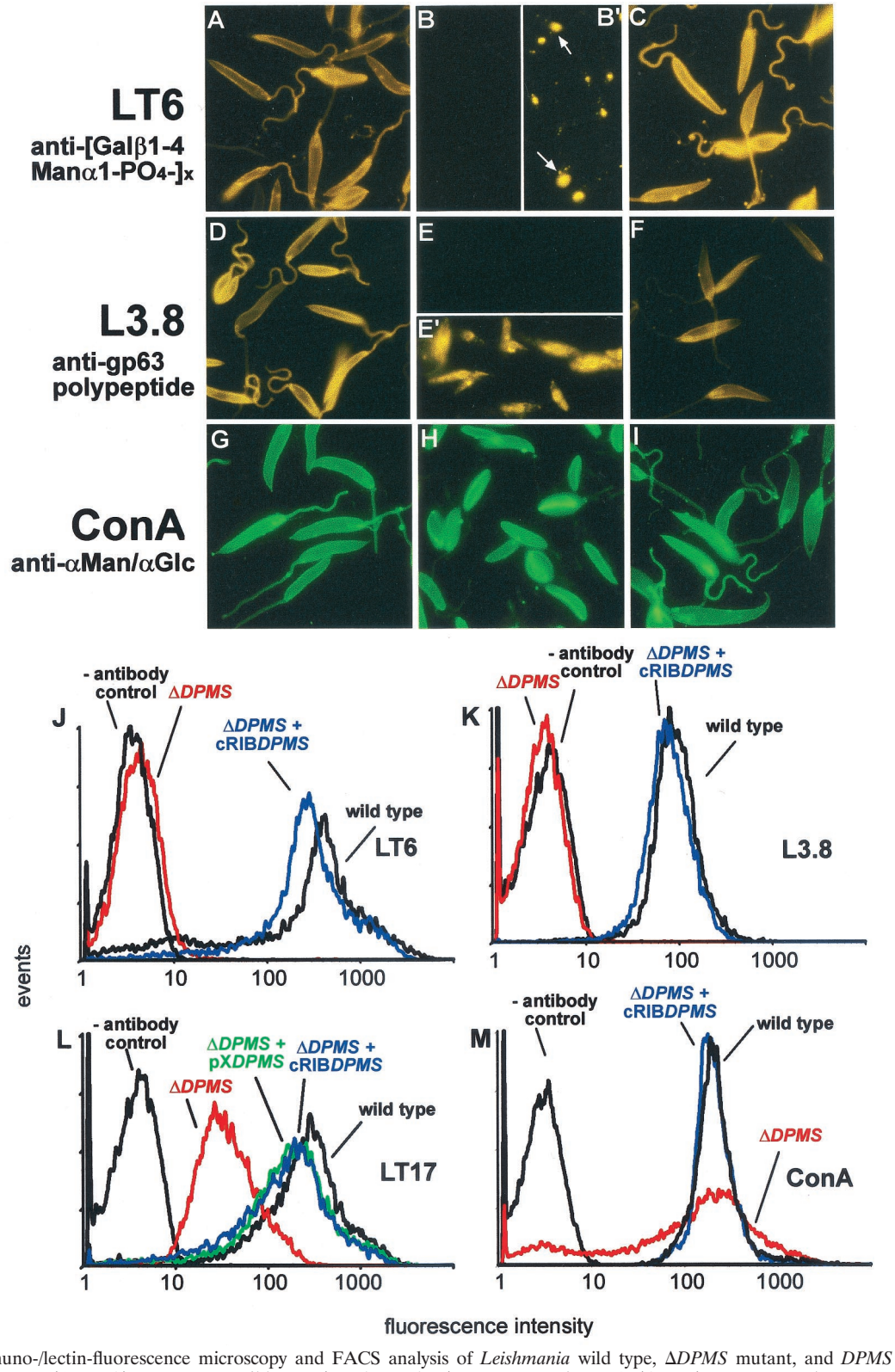

FIG. 10. Immuno-/lectin-fluorescence microscopy and FACS analysis of *Leishmania* wild type, Δ*DPMS* mutant, and *DPMS* gene addback mutant promastigotes. (A, D, G) *L. mexicana* wild type; (B, B′, E, E′, H) *L. mexicana* Δ*DPMS*; (C, F, I) *L. mexicana* Δ*DPMS* + cRIBΔ*DPMS*. Exposure times within rows are identical except for panels B′ and E′, which are approximately 20× overexposed compared to panels B and E, respectively. The cells were not permeabilized after fixation, except for panel E′, where the promastigotes were treated with 0.1% saponin throughout the labeling procedure. The MAbs and lectins used are indicated by the labeling of rows. The arrows in panel B′ indicate the positions of flagellar pockets. (J to M) FACS analysis of live *L. mexicana* promastigotes. The parasite lines and the MAbs and lectins used are indicated in each panel.

gesting localization in the endoplasmic reticulum (Fig. 10E′). [^{3}H]*myo*-inositol labeling of Δ*DPMS* promastigotes resulted in no incorporation of radioactive label into gp63 or any other *Leishmania* protein (Fig. 9C, lanes 1 and 2), suggesting that the biosynthesis of GPI anchors may be defective in the mutants. By contrast, N-glycosylation does not seem to be greatly affected in Δ*DPMS* cells, as the electrophoretic mobility of the membrane-bound acid phosphatase (MBAP), which carries up to eight N-glycans but is modified by neither phosphoglycans nor a GPI anchor (31), is largely unchanged (Fig. 9D, lanes 1 and 2).

Orcinol staining of HPTLC-separated total lipids suggests that the dominant Man-containing GIPLs iM2, iM3, and iM4 of wild-type parasites (Fig. 9E, lane 1; compare reference 30) are absent in *L. mexicana* Δ*DPMS* promastigotes (Fig. 9E, lane 2). This result was confirmed by [^{3}H]Man, [^{3}H]GlcNH_2 (Fig. 9F and G), and [^{3}H]*myo*-inositol (not shown) labelings, where these three glycolipids and EP-iM3 were undetectable in the mutant parasites.

The binding of ConA to the surface of Δ*DPMS* promastigotes was comparable to its binding to wild-type parasites, as indicated by immunofluorescence on fixed cells (Fig. 10G and H) and FACS analysis of live cells (Fig. 10M). By contrast, ricin, whose main ligand on *Leishmania* promastigotes is LPG (8), showed a strong signal on wild-type parasites, but a complete absence of lectin binding to the mutants was noted (data not shown). In hexose analysis, the Man content of *L. mexicana* Δ*DPMS* promastigote membranes was only about 3% of that detected in wild-type parasites (Fig. 6D).

Reexpression of the *DPMS* gene in Δ*DPMS* promastigotes either by integration into the ribosomal locus (Fig. 3B; Fig. 8A and C to F, lanes 3; Fig. 9C to G, lanes 3; Fig. 10C, F, I, and J to M) or by introduction of episomal gene copies (Fig. 10L and data not shown) led to the reversal of all protein and lipid glycosylation defects observed in the mutant parasites.

Attenuation and loss of virulence in *L. mexicana* Δ*DPMS* and Δ*PMM* mutants. *L. mexicana* Δ*PMM* promastigotes were unable to establish an infection in cultured macrophages (Fig. 11A). This inability was not due to a lack of attachment to and invasion of host cells, where the Δ*PMM* mutant proved to be as efficient than the *L. mexicana* wild type, but the invading parasites were killed soon after uptake (not shown). Furthermore, *L. mexicana* Δ*PMM* promastigotes proved to be avirulent to BALB/c mice, even at the high parasite dose (10^7/mouse) used in this study (Fig. 11B and C). Attempts to reisolate Δ*PMM* parasites from inoculated animals were repeatedly unsuccessful. Virulence of Δ*PMM* mutants to macrophages and mice could be restored by *PMM* gene addback either by chromosomal integration into the rRNA locus or by episome (Fig. 11A, B, and C). In contrast to these results, *L. mexicana* Δ*DPMS* unexpectedly still succeeded in colonizing the host cells and showed only a lowered infectivity to macrophages compared to wild-type parasites (Fig. 11D). In BALB/c mice, the onset and progression of disease was slightly slower compared to the wild-type strain, but the animals failed to control the infection, which led eventually to fatal disease (Fig. 11E). Δ*DPMS* parasites could be reisolated from lesion tissue, draining lymph nodes and the spleen of inoculated animals. The decrease in infectivity of the Δ*DPMS* mutant to macrophages and mice could be completely rescued by integrative or episomal *DPMS* gene addback (Fig. 11D and E).

DISCUSSION

The single-copy PMM gene of *L. mexicana* belongs to the same gene family as yeast and human PMMs and contains their conserved motifs and the active site aspartic acid. Expression of *L. mexicana* PMM in *E. coli* as an active enzyme and preliminary analysis of its properties suggest that in addition to a Manα1,6-bis-PO_4-dependent PMM activity, the enzyme also possesses a strong phosphoglucomutase activity (T. Ilg, unpublished results) similar to that of the yeast enzyme but unlike that of human PMM2. Given the essential functions of PMMs in yeast and humans, our finding that PMM gene deletion mutants of the eukaryotic parasite *L. mexicana* are viable in culture is remarkable. Although *L. mexicana* Δ*PMM* promastigotes still possess some PMM activity (<10%), possibly due to minor PMM activities of other mutases like phosphoglucomutase or phospho-*N*-acetylglucosaminemutase, this residual activity is not sufficient to rescue the parasite's profound glycosylation defects. A similar observation has been made for the *S. cerevisiae sec53* mutant, where two cytosolic PGMs unrelated to Sec53p possess strong PMM activity but are unable to rescue the lethal defect, even when overexpressed from a plasmid vector (2).

The lack of PMM activity in *L. mexicana* Δ*PMM* mutants leads to the suppression of protein and lipid glycosylation to such a degree that the Man content of their membranes is below the detection limit (less than 1% of wild-type levels) in the gas chromatography-mass spectrometry analysis employed in this study. Furthermore, GIPL expression is undetectable by radiolabeling techniques. Only sensitive immunochemical techniques and lectin binding assays detect a low level of expression of GPI-anchored gp63, mannooligosaccharide caps, and ConA binding sites in the Δ*PMM* mutants. The apparent discrepancy between an only 10-fold decrease in ConA binding in Δ*PMM* versus a more than 100-fold decrease in macromolecule-bound Man, as seen in the GC-MS analysis, may be explained by the fact that single terminal αMan residues in a glycosylation-defective, but leaky, Δ*PMM* mutant (e.g., Manα1-PO_4-Ser on PPGs) may still be ligands for ConA molecules (and MAb L7.25, T. Ilg, unpublished data) while in the wild type many of the ConA binding structures are Man-rich phosphoglycan chains terminating in mannooligosaccharides ([Manα1-2]$_{0\text{-}5}$Man; Fig. 1A). This may lead to a nonlinear relationship between the Man content of *Leishmania* macromolecules and ConA binding. Cross-reaction or nonspecific binding of ConA to other structures is considered unlikely, as the nonleaky GDPMP gene deletion mutant (Δ*GDPMP*) does not show the low ConA signal observed on Δ*PMM* promastigotes (12). The low level of leakiness of Δ*PMM* parasites may be explained by the synthesis of very limited amounts of Manα1-PO_4 via their residual PMM activity. In contrast to the Δ*PMI* mutants characterized in an earlier study (11), the glycosylation and growth defects of Δ*PMM* cannot be rescued by exogenous Man. This inability of the Δ*PMM* parasites to utilize exogenous Man for glycoconjugate synthesis may explain their failure to colonize macrophages or mice, while the Δ*PMI* parasites having this capacity remain infectious (11).

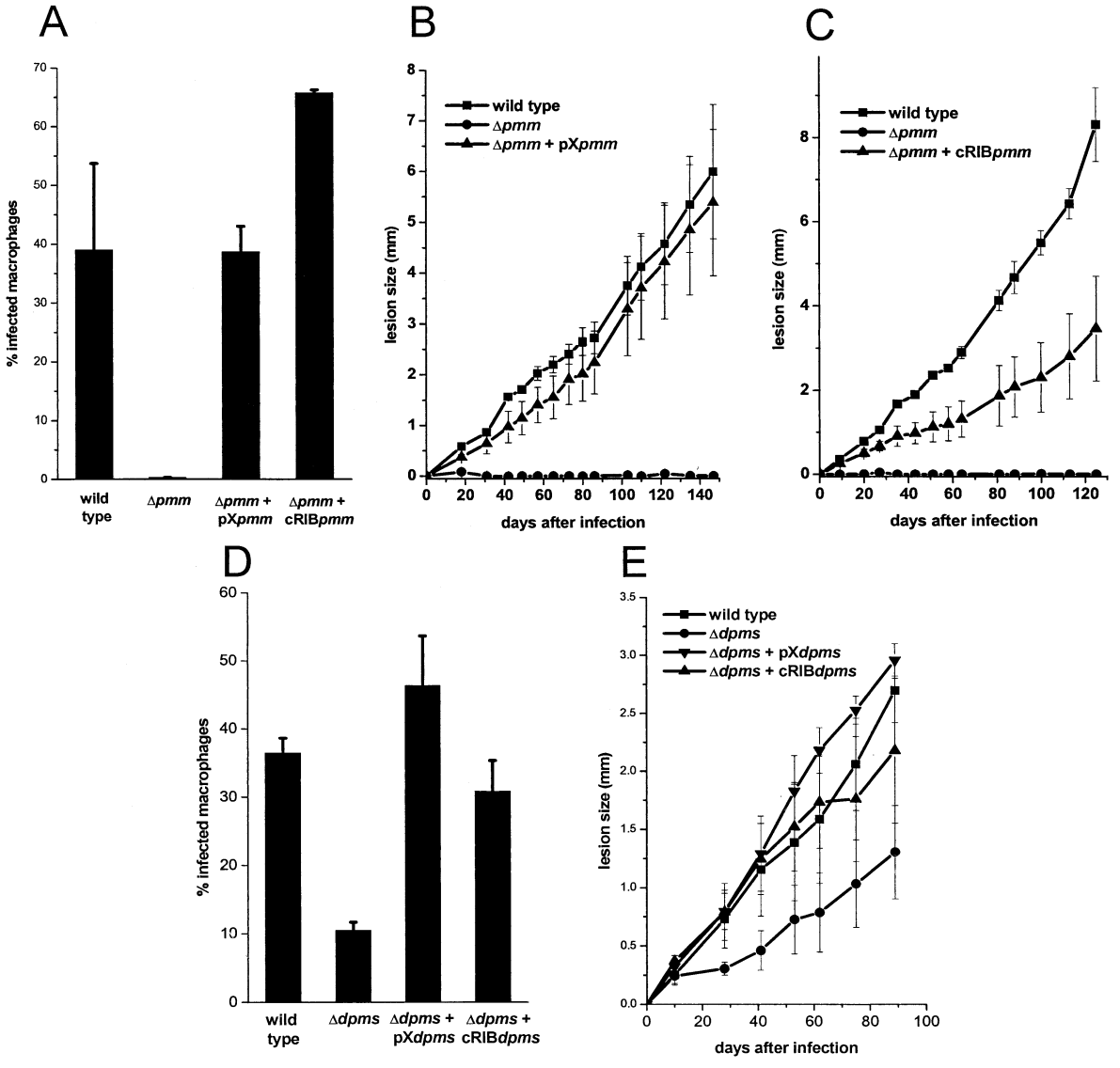

FIG. 11. Analysis of macrophage and mouse infections by *L. mexicana* wild type and mutants. (A, D) Infection of peritoneal macrophages by *L. mexicana* wild type, Δ*PMM*, Δ*PMM* + pX*PMM*, Δ*PMM* + cRIB*PMM* (A) or by *L. mexicana* wild type, Δ*DPMS*, Δ*DPMS* + pX*DPMS*, Δ*DPMS* + cRIB*DPMS* (D). Peritoneal macrophages were infected at a ratio of two stationary phase promastigotes per cell. The percentage of infected macrophages (sample size, 300) was counted 6 days after the infection. The standard errors of duplicate experiments are indicated. (B, C, E) For in vivo infection experiments, BALB/c mice were challenged with 10^7 *L. mexicana* promastigotes in the right hind footpad. The swelling caused by *L. mexicana* wild type, Δ*PMM*, and Δ*PMM* + pX*PMM* (B), by *L. mexicana* wild type, Δ*PMM*, and Δ*PMM* + cRIB*PMM* (C), and by *L. mexicana* wild type, Δ*DPMS*, Δ*DPMS* + pX*DPMS*, or Δ*DPMS* + pRIB*DPMS* (E) was recorded. The infection experiments were performed in quadruplicates and the standard error is indicated.

L. mexicana DPMS is an enzyme associated with the endoplasmic reticulum, which has been reported to be essential for the parasites (22). However, the existence of a *L. mexicana* mutant lacking the PMM gene suggested that, in conflict with this view, DPMS may not be required for *L. mexicana* viability. This prediction was confirmed by the generation of parasite clones lacking the DPMS ORF (Δ*DPMS*) and lacking detectable DPMS activity. *L. mexicana* Δ*DPMS* promastigotes are unable to express LPG, Man-containing GIPLs, and the GPI-anchored surface metalloproteinase leishmanolysin (gp63). Given the fact that *L. mexicana* Δ*DPMS* lack the three surface glycoconjugates LPG, gp63, and GIPLs, which have been described as major virulence factors in *Leishmania* (3, 8, 38), the infectivity of this particular mutant to macrophages and mice is very surprising. While it has been shown previously that surface expression of LPG and gp63 is downregulated to undetectable levels in *L. mexicana* amastigotes (17, 18), the Man-containing GIPLs are highly abundant in this disease-causing *Leishmania* life stage (42). Therefore, these glycolipids in particular were generally perceived as being crucial molecules for parasite survival and virulence to the mammalian host (8, 22, 42). However, in contrast to this expectation, the disease that large doses of the mutant parasites elicit in mice is, after an initial lag phase, as severe as that caused by wild-type parasites. Whether lower doses of *L. mexicana* Δ*DPMS* promastigotes lead to more pronounced differences in virulence to mice, as

TABLE 1. Glycosylation defects and virulence phenotypes of *L. mexicana* mutants

L. mexicana line	Virulence to macrophages and mice[a]	Defect(s) in glycoconjugate synthesis	Reference(s)
WT	++	Normal expression of all Man-containing glycoconjugates (LPG., PPGs, protein GPIs, Man-containing GIPIs, N-glycans)	This study; 12, 15, 16, 21
Δ*lmexlpg1*	++	No expression of LPG	16
Δ*lmexlpg2*	++	No expression of LPG and no phosphoglycosylation of PPGs (except for small amounts of PPG manno-oligosaccharide caps)	21
Δ*GPI18*	++	No expression of protein GPIs	15
Δ*GDPMP*	−	No expression of LPG, protein GPIs, Man-containing GIPLs and N-glycans, and no phosphoglycosylation of PPGs	12
Δ*PMM*	−	Severely downregulated expression of LPG, protein GPIs, Man-containing GIPLs, and N-glycans, and downregulated phosphoglycosylation of PPGs	This study
Δ*DPMS*	+	No expression of LPG, protein GPI anchors, and Man-containing GIPLs	This study

[a] ++, fully virulent (no difference to wild type); +, virulent, but attenuated (lower efficiency of infection); −, avirulent (no infectivity).

indicated by the lower efficiency of colonization of in vitro-cultured macrophages compared to wild-type parasites observed in this study, is presently being assessed.

For *L. mexicana*, a comprehensive picture of the significance of Man-containing glycoconjugates for parasite virulence starts to emerge (Table 1): we have shown earlier that LPG alone is not required for full virulence of *L. mexicana* (16). The absence of GPI-anchored proteins, including gp63 (15), and the lack of LPG and PPGs (21) is not abrogating virulence to mammals either. In this study, we have shown that even the combined absence of LPG, GPI-anchored gp63, and Man-containing GIPLs in *L. mexicana* Δ*DPMS* does not lead to loss of infectivity. Only the drastically downregulated expression of all known Man-containing glycoconjugates in the *L. mexicana* Δ*PMM* mutant leads to an avirulent phenotype. These results have recently been confirmed by our studies on the GDPMP of *L. mexicana* (Table 1) (12). Δ*GDPMP* mutants of this species are viable and lack Man-containing glycoconjugates, and even the residual levels detected by immunochemical reagents in Δ*PMM* mutants are absent in this parasite line. Like the Δ*PMM* parasites, Δ*GDPMP L. mexicana* parasites are unable to infect in vitro-cultured macrophages or mice (12).

What are now the glycan components required for virulence? In contrast to the avirulent Δ*PMM* and Δ*GDPMP* mutants, the virulent Δ*DPMS* parasites exhibit a normal capacity to synthesize PPG phosphoglycan repeats and caps, and N-glycosylation appears to be largely unaffected. On the other hand, however, the virulent Δ*lmexlpg2* mutant lacks phosphoglycans on PPGs, except for small numbers of mannooligosaccharide cap epitopes (Table 1) (21). This leaves the latter structures and N-glycans on the agenda as potential virulence determinants. Alternatively, it is conceivable that within the five different classes of *Leishmania* glycoconjugates (LPG, PPGs, protein GPIs, GIPLs, and N-glycans) with respect to infectivity, functional cross-compensation for the loss of one, two, or even three classes may be possible, but the loss of all classes is not tolerated. In any case, our study suggests that the virulence phenotype of *Leishmania* cannot be pinned down to a single Man-containing glycoconjugate virulence factor and there may be considerable functional redundancy within these classes of parasite molecules. However, Man activation to GDP-Man in *Leishmania* (Fig. 1B) emerges from this and another recent study (12) as a virulence pathway and it appears to be worthwhile to explore *Leishmania* PMM as a potential target for the development of new anti-parasite drugs.

ACKNOWLEDGMENTS

We thank Suzanne Gokool and Peter Overath for thoughtful suggestions on the manuscript, Kinga Harsányi for help with the gene cloning, and Dorothee Harbecke and Monika Demar for expert technical assistance.

REFERENCES

1. **Beverley, S. M., and S. J. Turco.** 1998. Lipophosphoglycan (LPG) and the identification of virulence genes in the protozoan parasite *Leishmania.* Trends Microbiol. **6:**35–40.
2. **Boles, E., W. Liebetrau, M. Hofmann, and F. K. Zimmermann.** 1994. A family of hexosephosphate mutases in *Saccharomyces cerevisiae.* Eur. J. Biochem. **220:**83–96.
3. **Brittingham, A., C. J. Morrison, W. R. McMaster, B. S. McGwire, K. P. Chang, and D. M. Mosser.** 1995. Role of the *Leishmania* surface protease gp63 in complement fixation, cell adhesion, and resistance to complement-mediated lysis. J. Immunol. **15:**3102–3111.
4. **Collet, J., V. Strooban, M. Pirard, G. Delpierre, and E. Van Schaftingen.** 1998. A new class of phosphotransferases phosphorylated on an aspartate residue in an amino-terminal DXDX(T/V) motif. J. Biol. Chem. **273:**14107–14112.
5. **Colussi, P. A., C. H. Taron, J. C. Mack, and P. Orlean.** 1997. Human and *Saccharomyces cerevisiae* dolichol phosphate mannose synthases represent two classes of the enzyme, but both function in *Schizosaccharomyces pombe.* Proc. Natl. Acad. Sci. USA **94:**7873–7878.
6. **Cruz, A., C. M. Coburn, and S. M. Beverley.** 1991. Double targeted gene replacement for creating null mutants. Proc. Natl. Acad. Sci. USA **89:**7170–7174.
7. **Cummings, R. D.** 1999. Plant lectins, p. 455–467. *In* A. Varki, R. Cummings, J. Esko, H. Freeze, G. Hart, and J. Marth (ed.), Essentials of glycobiology. Cold Spring Harbor Laboratory Press, Cold Spring Harbor, N.Y.
8. **Descoteaux, A., and S. J. Turco.** 1999. Glycoconjugates in *Leishmania* infectivity. Biochim. Biophys. Acta **1455:**341–352.
9. **Ferguson, M. A. J.** 1992. GPI membrane anchors: isolation and analysis, p. 349–383. *In* M. Fukuda and A. Kobata (ed.), Glycobiology, a practical approach. IRL Press, Oxford, United Kingdom.
10. **Ferguson, M. A. J.** 1999. The structure, biosynthesis and functions of glycosylphosphatidylinositol anchors, and the contributions of trypanosome research. J. Cell Sci. **112:**2799–2809.
11. **Garami, A., and T. Ilg.** 2001. The role of phosphomannose isomerase in *Leishmania mexicana* glycoconjugate synthesis and virulence. J. Biol. Chem. **276:**6566–6575.
12. **Garami, A., and T. Ilg.** 2001. Disruption of mannose activation in *Leishmania mexicana*: GDP-mannose pyrophosphorylase is required for virulence, but not for viability. EMBO J. **20:**3657–3666.
13. **Göpfert, U., N. Goehring, C. Klein, and T. Ilg.** 1999. Proteophosphoglycans of *Leishmania mexicana*. Molecular cloning and characterization of the *Leishmania mexicana ppg2* gene encoding the proteophosphoglycans aPPG and pPPG2 that are secreted by amastigotes and promastigotes. Biochem. J. **344:**787–795.
14. **Hashimoto, H., A. Sakakibara, M. Yamasaki, and K. Yoda.** 1997. *Saccharomyces cerevisiae* VIG9 encodes GDP-mannose pyrophosphorylase, which is essential for protein glycosylation. J. Biol. Chem. **272:**16308–16314.
15. **Hilley, J. D., J. L. Zawadzki, M. J. McConville, G. H. Coombs, and J. C. Mottram.** 2000. *Leishmania mexicana* mutants lacking glycosylphosphatidylinositol (GPI):protein transamidase provide insights into the biosynthesis and functions of GPI-anchored proteins. Mol. Biol. Cell **11:**1183–1195.
16. **Ilg, T.** 2000. Lipophosphoglycan is not required for infection of macrophages or mice by *Leishmania mexicana.* EMBO J. **19:**1–11.

17. **Ilg, T.** 2000. Proteophosphoglycans of *Leishmania.* Parasitol. Today **16:**489–497.
18. **Ilg, T., D. Harbecke, and P. Overath.** 1993. The lysosomal gp63-related protein in *Leishmania mexicana* amastigotes is a soluble metalloproteinase with an acidic pH optimum. FEBS Lett. **327:**103–107.
19. **Ilg, T., D. Harbecke, M. Wiese, and P. Overath.** 1993. Monoclonal antibodies directed against *Leishmania* secreted acid phosphatase and lipophosphoglycan. Partial characterization of private and public epitopes. Eur. J. Biochem. **217:**603–615.
20. **Ilg, T., J. Montgomory, Y.-D. Stierhof, and E. Handman.** 1999. Molecular cloning and characterization of a novel repeat-containing *Leishmania major* gene, *ppg1*, that encodes a membrane-associated form of proteophosphoglycan with a putative glycosylphosphatidylinositol anchor. J. Biol. Chem. **274:** 31410–31420.
21. **Ilg, T., M. Demar, and D. Harbecke.** 2001. Phosphoglycan repeat-deficient *Leishmania mexicana* parasites remain infectious to macrophages and mice. J. Biol. Chem. **276:**4988–4997.
22. **Ilgoutz, S. C., J. L. Zawadzki, J. E. Ralton, and M. J. McConville.** 1999. Evidence that free GPI glycolipids are essential for growth of *Leishmania mexicana.* EMBO J. **18:**2746–2755.
23. **Kepes, F., and R. Schekman.** 1988. The yeast SEC53 gene encodes phosphomannomutase. J. Biol. Chem. **263:**9155–9161.
24. **LeBowitz, J. H., C. M. Coburn, D. McMahon-Pratt, and S. M. Beverley.** 1990. Development of a stable *Leishmania* expression vector and application to the study of parasite surface antigen genes. Proc. Natl. Acad. Sci. USA **87:**9736–9740.
25. **Maeda, Y., S. Tomita, R. Watanabe, K. Ohishi, and T. Kinoshita.** 1998. DPM2 regulates biosynthesis of dolichol phosphate-mannose in mammalian cells: correct subcellular localization and stabilization of DPM1, and binding of dolichol phosphate. EMBO J. **17:**4920–4929.
26. **Maeda, Y., S. Tanaka, J. Hino, K. Kangawa, and T. Kinoshita.** 2000. Human dolichol-phosphate-mannose synthase consists of three subunits, DPM1, DPM2 and DPM3. EMBO J. **19:**2475–2482.
27. **Matthijs, G., E. Schollen, M. Pirard, M. L. Budarf, E. Van Schaftingen, and J. Cassiman.** 1997. PMM (PMM1), the human homologue of sec53 or yeast phosphomannomutase, is localized on chromosome 22q13. Genomics **40:**41–47.
28. **Matthijs, G., E. Schollen, E. Pardon, M. Veiga-Da-Cunha, J. Jaeken, J. J. Cassiman, and E. Van Schaftingen.** 1997. Mutations in PMM2, a phosphomannomutase gene on chromosome 16p13, in carbohydrate-deficient glycoprotein type I syndrome (Jaeken syndrome). Nat. Genet. **16:**88–92.
29. **McConville, M. J., J. E. Thomas-Oates, M. A. Ferguson, and S. W. Homans.** 1990. Structure of the lipophosphoglycan from *Leishmania major.* J. Biol. Chem. **265:**19611–19623.
30. **McConville, M. J., T. A. Collidge, M. A. J. Ferguson, and P. Schneider.** 1993. The glycoinositol phospholipids of *Leishmania mexicana* promastigotes. Evidence for the presence of three distinct pathways of glycolipid biosynthesis. J. Biol. Chem. **268:**15595–15604.
31. **Menz, B., G. Winter, T. Ilg, F. Lottspeich, and P. Overath.** 1991. Purification and characterization of a membrane-bound acid phosphatase of *Leishmania mexicana.* Mol. Biochem. Parasitol. **47:**101–108.
32. **Oesterhelt, C., C. Schnarrenberger, and W. Gross.** 1997. The reaction mechanism of phosphomannomutase in plants. FEBS Lett. **401:**35–37.
33. **Orlean, P., C. Albright, and P. W. Robbins.** 1988. Cloning and sequencing of the yeast gene for dolichol phosphate mannose synthase, an essential protein. J. Biol. Chem. **263:**17499–17507.
34. **Orlean, P.** 2000. Congenital disorders of glycosylation caused by defects in mannose addition during N-linked oligosaccharide assembly. J. Clin. Investig. **105:**131–132.
35. **Peterson, G. L.** 1983. Determination of total protein. Methods Enzymol. **91:**95–119.
36. **Pirard, M., Y. Achouri, J. F. Collet, E. Schollen, G. Matthijs, and E. Van Schaftingen.** 1999. Kinetic properties and tissular distribution of mammalian phosphomannomutase isoenzymes. Biochem. J. **339:**201–207.
37. **Pirard, M., G. Matthijs, L. Heykants, E. Schollen, S. Grunewald, J. Jaeken, and E. Van Schaftingen.** 1999. Effect of mutations found in carbohydrate-deficient glycoprotein syndrome type IA on the activity of phosphomannomutase 2. FEBS Lett. **452:**319–322.
38. **Proudfoot, L., C. A. O'Donnell, and F. Y. Liew.** 1995. Glycoinositolphospholipids of *Leishmania major* inhibit nitric oxide synthesis and reduce leishmanicidal activity in murine macrophages. Eur. J. Immunol. **25:**745–750.
39. **Stierhof, Y.-D., T. Ilg, D. G. Russell, H. Hohenberg, and P. Overath.** 1994. Characterization of polymer release from the flagellar pocket of *Leishmania mexicana* promastigotes. J. Cell Biol. **125:**321–331.
40. **Wiese, M., T. Ilg, F. Lottspeich, and P. Overath.** 1995. Ser/Thr-rich repetitive motifs as targets for phosphoglycan modifications in *Leishmania mexicana* secreted acid phosphatase. EMBO J. **14:**1067–1074.
41. **Wiese, M., O. Berger, Y.-D. Stierhof, M. Wolfram, M. Fuchs, and P. Overath.** 1996. Gene cloning and cellular localization of a membrane-bound acid phosphatase of *Leishmania mexicana.* Mol. Biochem. Parasitol. **25:**153–165.
42. **Winter, G., M. Fuchs, M. J. McConville, Y.-D. Stierhof, and P. Overath.** 1994. Surface antigens of *Leishmania mexicana* amastigotes: characterization of glycoinositol phospholipids and a macrophage-derived glycosphingolipid. J. Cell Sci. **107:**2471–2482.